

We are IntechOpen, the world's leading publisher of Open Access books Built by scientists, for scientists

6,900

Open access books available

185,000

International authors and editors

200M

Downloads

Our authors are among the

154

Countries delivered to

TOP 1%

most cited scientists

12.2%

Contributors from top 500 universities



WEB OF SCIENCE™

Selection of our books indexed in the Book Citation Index
in Web of Science™ Core Collection (BKCI)

Interested in publishing with us?
Contact book.department@intechopen.com

Numbers displayed above are based on latest data collected.
For more information visit www.intechopen.com



Analysis of Platform Noise Effect on Performance of Wireless Communication Devices

Han-Nien Lin
Feng-Chia University
Taiwan, R.O.C.

1. Introduction

Cloud computation and always-connected Internet attracts the most industrial attention for the past few years. Meanwhile, with the development of IC technologies advancing toward higher operating frequencies and the trend of miniaturization on wireless communication products, the circuits and components are placed much closer inside the wireless communications devices than ever before. The system with highly integrated high-speed digital circuits and multi-radio modules are now facing the challenge from performance degradation by even more complicated platform EMI noisy environment. The EMI noises emitted by unintentionally radiated interference sources may severely impact the receiving performance of antenna, and thus result in the severe performance degradation of wireless communications. Due to the miniaturization of a variety of wireless communications products, the layout and trace routing of circuits and components become much denser than ever before. Therefore, we have investigated and analyzed the EMI noise characteristics of commonly embedded digital devices for further high performance wireless communications design. Since the camera and display module is most adopted to the popular mobile devices like cellular phone or Netbook, we hence focus on EMI analysis of the built-in modules by application of IEC 61967[1][2] series measurement method.

Since the causes of reduction of throughput or coverage due to receiving sensitivity degradation of wireless system could result from decreased S/N via conducted or radiated EMI noises from nearby digital components shown in Figure 1. This chapter discusses RF de-sensitivity analysis for components and devices on mobile products. To improve the TIS performance of wireless communication on notebook computer, we investigated the EMI noise from the built-in camera and display modules as examples and analysed the impact of various operation modes on performance with throughput measurement. We also utilized the near-field EM surface scanner to detect the EMI sources on notebook and locate the major noisy sources around antenna area. From the emission levels and locations of the noisy components, we can then figure out their impact on throughput and receiving sensitivity of wireless communications and develop the solutions to improve system performance. Finally, we designed and implemented periodic structures for isolation on the

notebook computer to effectively suppress noise source-antenna coupling and improve the receiving sensitivity of wireless communication system.

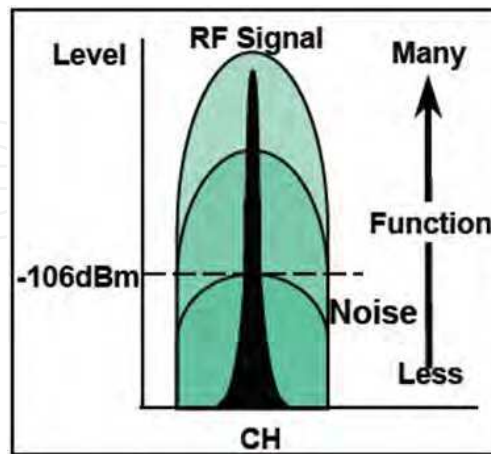


Fig. 1. S/N ratio decreases due to digital components for multi-functions.

2. The noise impact of camera and Touch Panel (TP) modules on product performance

2.1 Performance testing for Wireless Wide Area Network (WWAN) devices

There are two different purposes for the OTA (Over-The-Air) testing[3] on mobile stations. The first testing is for the carrier's cell site coverage which is relative with loss plan and link budget of the cell site. For example, the sensitivity measurement of the W-CDMA receiver is performed by the base-station simulator to determine the receiving sensitivity of EUT (Equipment Under Test) by reporting the minimum forward-link power which resulting in a bit-error-rate (BER) of 1.2% or less at the data rate of 12.2 kbps with a minimum of 20,000 bits. The second testing is the throughput for supporting all kind of the applications for cloud computing. The minimum throughput required will depend on application. For example, the minimum throughput we need to link YOU TUBE for HD video is about 1Mbps at least. Therefore, the mobile station (Smart Phone, Tablet PC, Note book PC, etc.) is required the OTA performance testing on TRP, TIS and De-Sense.

2.1.1 Total Radiated Power (TRP)

TRP measurement is to evaluate the transmitting RF power performance of mobile device by summing the effective isotropic radiated power (EIRP) of complete Theta- and Phi-cut as shown in Figure 2. The procedure is first to measure the radiated power at each Phi degree interval for 360 degree rotation (if interval is 30 degree then it need 12 measurement), and then for the Theta axial. Finishing the 180 degree rotation along Theta axial, the TRP is obtained with following formula.

$$TRP \cong \frac{\pi}{2NM} \sum_{i=1}^{N-1} \sum_{j=0}^{M-1} [EiRP_{\theta}(\theta_i, \phi_j) + EiRP_{\phi}(\theta_i, \phi_j)] \sin(\theta_i) \quad (1)$$

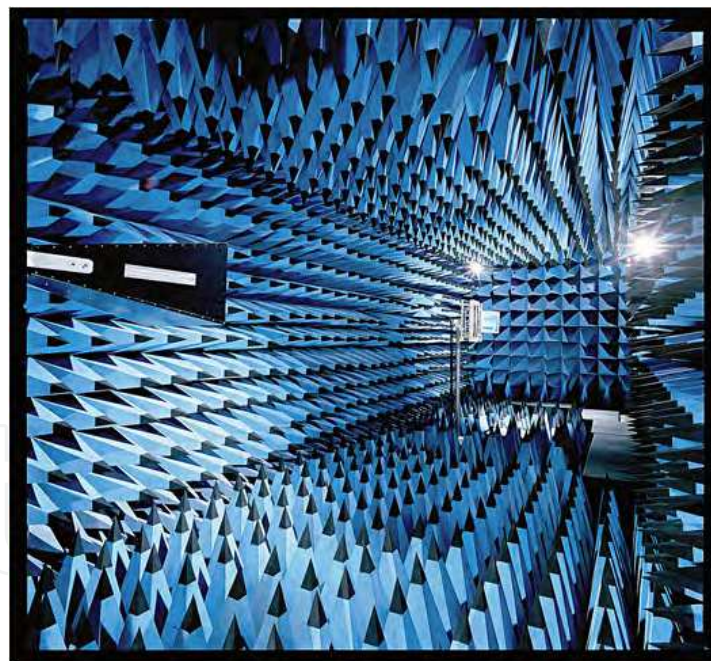
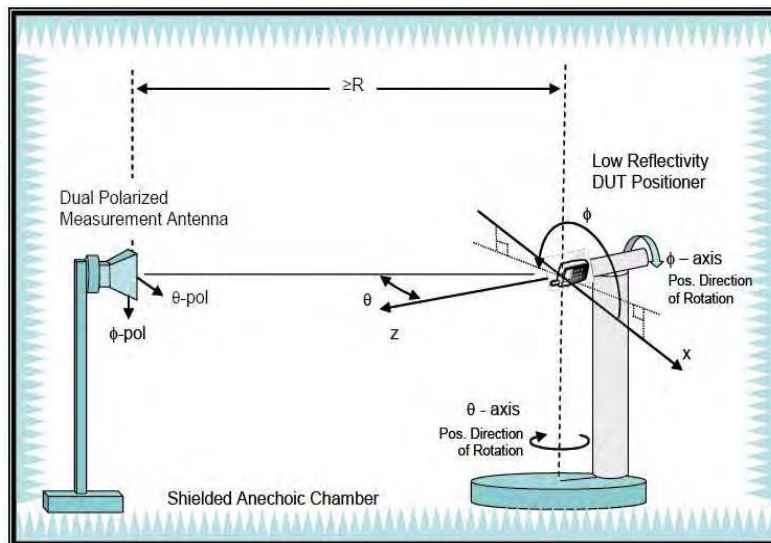


Fig. 2. Total Radiated Power measurement.

For the ideal case, the TRP should be equal to the conducted power (Watts) times mismatching Loss (%) and antenna efficiency as shown in following relationship and illustration. But the antenna efficiency measurement can actually with error resulting from coaxial cable connection as illustrated in Figure 3. When the coaxial cable is connected to the SMA connector, the surface on it could cause measurement error of the antenna efficiency.

$$TRP = \frac{1}{4\pi} \int_{\theta=0}^{\pi} \int_{\phi=0}^{2\pi} (EiRP_{\theta}(\theta, \phi) + EiRP_{\phi}(\theta, \phi)) \sin(\theta) d\theta d\phi$$

$$TRP = P_A \cdot L_m \cdot eff \tag{2}$$

Transmit Power = Pc (Conducted Power) + Antenna Gain (in dB)

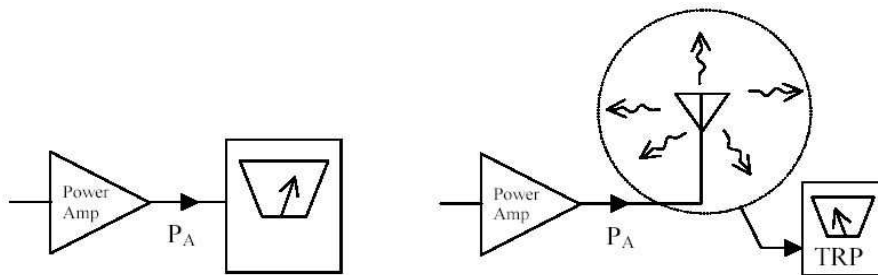
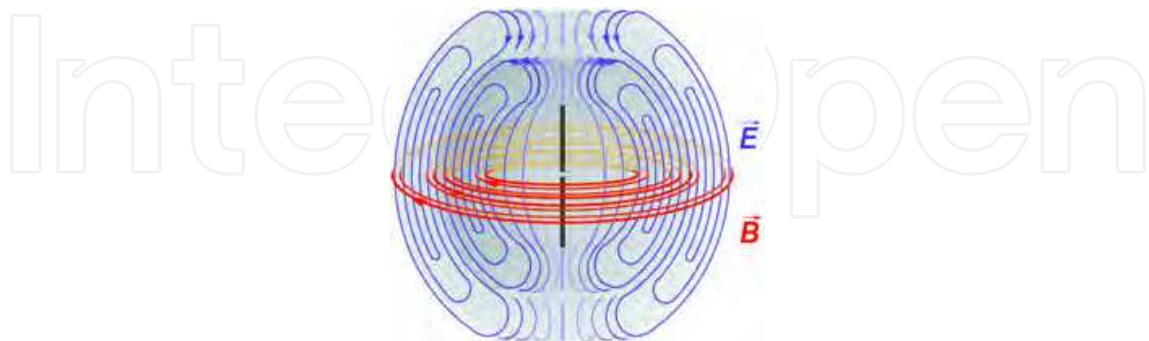


Fig. 3. Illustration of Antenna TRP.

2.1.2 Total Isotropic Sensitivity (TIS)

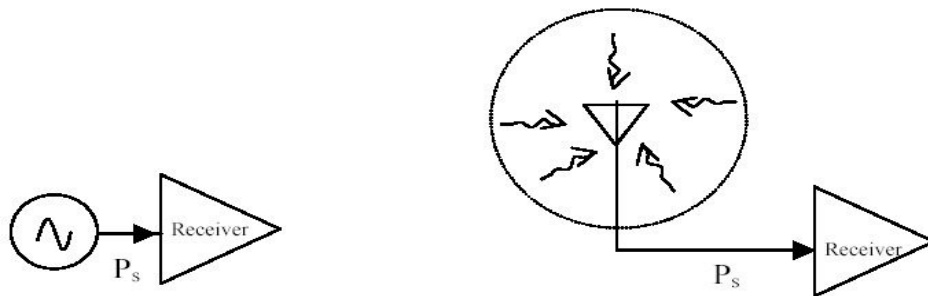
The measurement setup for TIS testing is the same as shown in Figure 2, except with the different calculation. It is analogous to calculate the total resistance form the parallel resistor network. The Effective Isotropic Sensitivity (EIS) is illustrated in Figure 4 and calculated with following formula.

$$TIS \cong \frac{2NM}{\pi \sum_{i=1}^{N-1} \sum_{j=0}^{M-1} \left[\frac{1}{EIS_{\theta}(\theta_i, \phi_j)} + \frac{1}{EIS_{\phi}(\theta_i, \phi_j)} \right] \sin(\theta_i)} \tag{3}$$

$$G_{x,EUT}(\theta, \phi) = \frac{P_s}{EIS_x(\theta, \phi)} \tag{4}$$

$$TIS = \frac{4\pi}{\oint \left[\frac{1}{EIS_{\theta}(\theta, \phi)} + \frac{1}{EIS_{\phi}(\theta, \phi)} \right] \sin(\theta) d\theta d\phi} \tag{5}$$

For the ideal case, TIS should be equal to conductive sensitivity divided by mismatching loss and antenna efficiency as shown in following relationship and illustration. Not only the surface current on coaxial cable would cause the antenna efficiency measurement error, but also the platform noise interference investigated here would de-sense the receiver.



EIS: Effective Isotropic Sensitivity = Received EIRP - Antenna Gain (in dB)
 TIS: Total Isotropic Sensitivity (3D Measurement)

Fig. 4. Illustration of Antenna TIS.

The relationship between receiver performance and platform noise is described by receiver bit error rate and energy per bit (E_b) / Noise(N_0) as shown in Figure 5. For example, the WCDMA receiver sensitivity with QPSK modulation can be determined as following:

Bit Error Rate (BER): 1.2% BER for QPSK demodulation receiver require that $E_b/N_0 = 7.5\text{dB}$

where E_b : measured at base-band output (I/Q output) for each bit.

N_0 : total noise power form RF front end to base-band, include LNA NF, ADC, quantize noise, PLL phase Noise,...with Gaussian system noise representation.

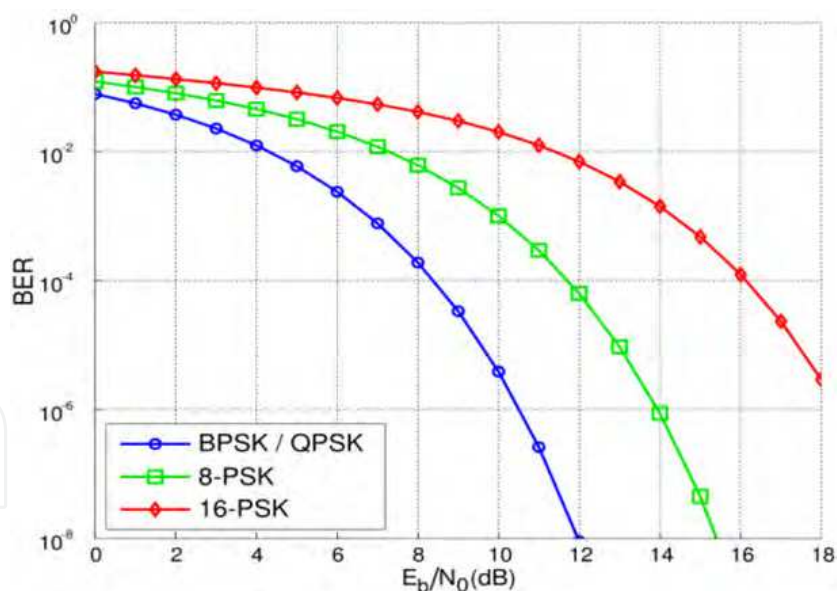


Fig. 5. Receiver Bit Error Rate vs. Energy per bit (E_b) / Noise(N_0).

The BER is measured in time domain after demodulation of receiver. For WCDMA system, it needs $20\text{k bits} / 12.2\text{Kbps} = 1.64$ second at each receiving channel. From communication demodulation theory, N_0 is described as Gaussian noise, and it is the sum of the receiver noise (related to implementation loss) and system noise as illustrated in the following figures.

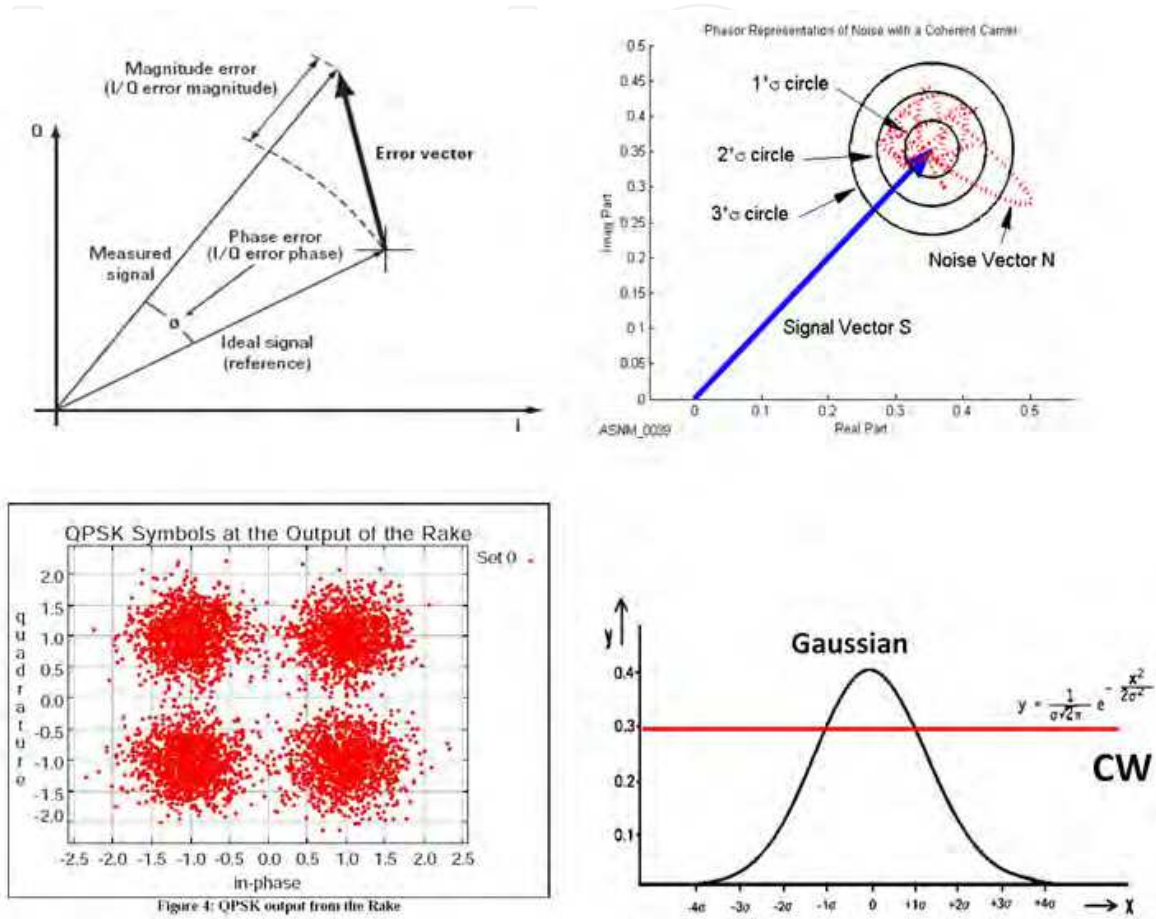


Fig. 6. Illustration of system noise effect.

Based on TIS requirement for WWAN or WLAN throughput, the noise limit of the wireless system should be set to meet the regulatory specification. Figure 7 shows the sensitivity degradation due to self-interference for GSM 1800 and WCDMA systems. The example for WCDMA system is following:

Noise Limit: TIS (dBm) + Antenna Gain (dB) - E_b/N_0 (dB) + Processing Gain (demodulation dependence) - System Losses (6dB) (depending on chip set, LNA NF, PLL phase noise, ADC.....), Processing Gain (dB)=10 Log(Chip rate/Data Rate) = 10log (3840K/12.2K)= 25dB

WCDMA Noise Limit : Gaussian Probability Density Function Noise Power-103dBm + (-5dB) -7.5dB +25dB - 6dB = 96.5dBm

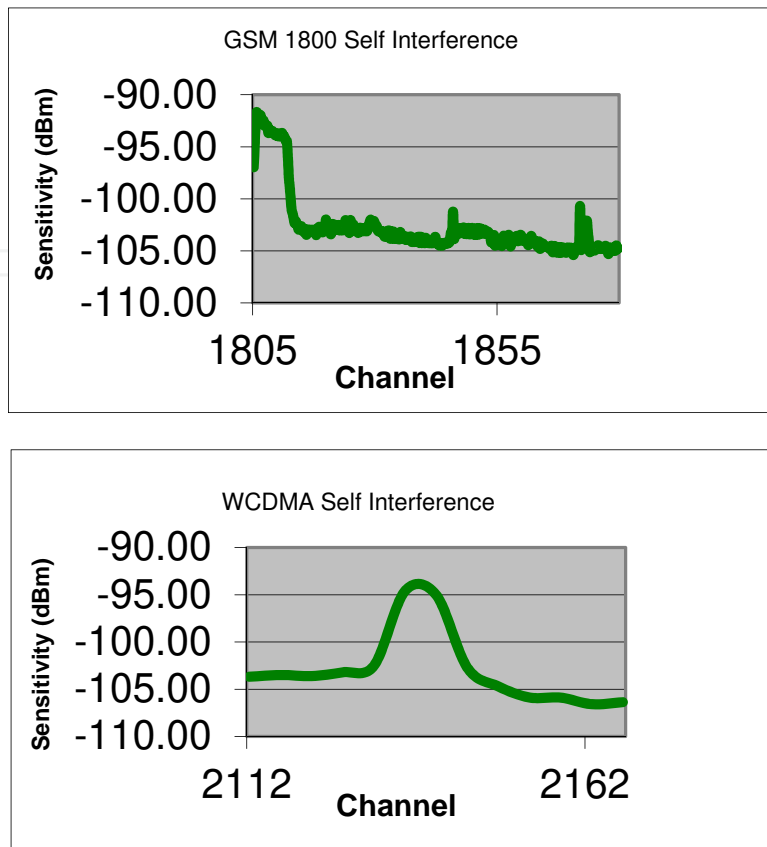


Fig. 7. Sensitivity degradation examples for GSM 1800 and WCDMA systems.

However, since there are more than one thousand Channels for GSM and WCDMA systems, we can't test all receiving channels for those WWAN devices. The alternative way for testing those intermediate channels is to measure the relative sensitivity as following steps and illustration as shown in Figure 8:

1. Move the EUT and position to the location and polarization which results in best radiated sensitivity, then measure for the closest channel (in frequency) and set as Reference Channel. After the 3D testing of the high, middle and lower channels (set as reference channel), we acn then review the 3D graph and find the best sensitivity at theta- and phi-plane of EIS along vertical or norizontal polarization (it means the best radiated sensitivity).
2. Now, there are three bset radiated sensitivity at Theta- and Phi-polarization for Low, Middle and High reference channel in one band. The rest of channels in one band should be then tested as following: The all channels in frequency range from lowest frequency channel (reference channel) to the frequency at $(\text{low} + \text{Middle})/2$ should be de-sensed less than 5 dB to the reference channel. The all channels in middle band of frequency from $(\text{Low} + \text{Middle})/2$ to $(\text{Middle} + \text{High})/2$ should be de-sensed less than 5dB to the reference channel (middle channel). Finally, the all channels in high band of frequency from $(\text{Middle} + \text{High}) / 2$ to (High should be de-sensed less than 5dB to the reference channel (highest frequency channel).

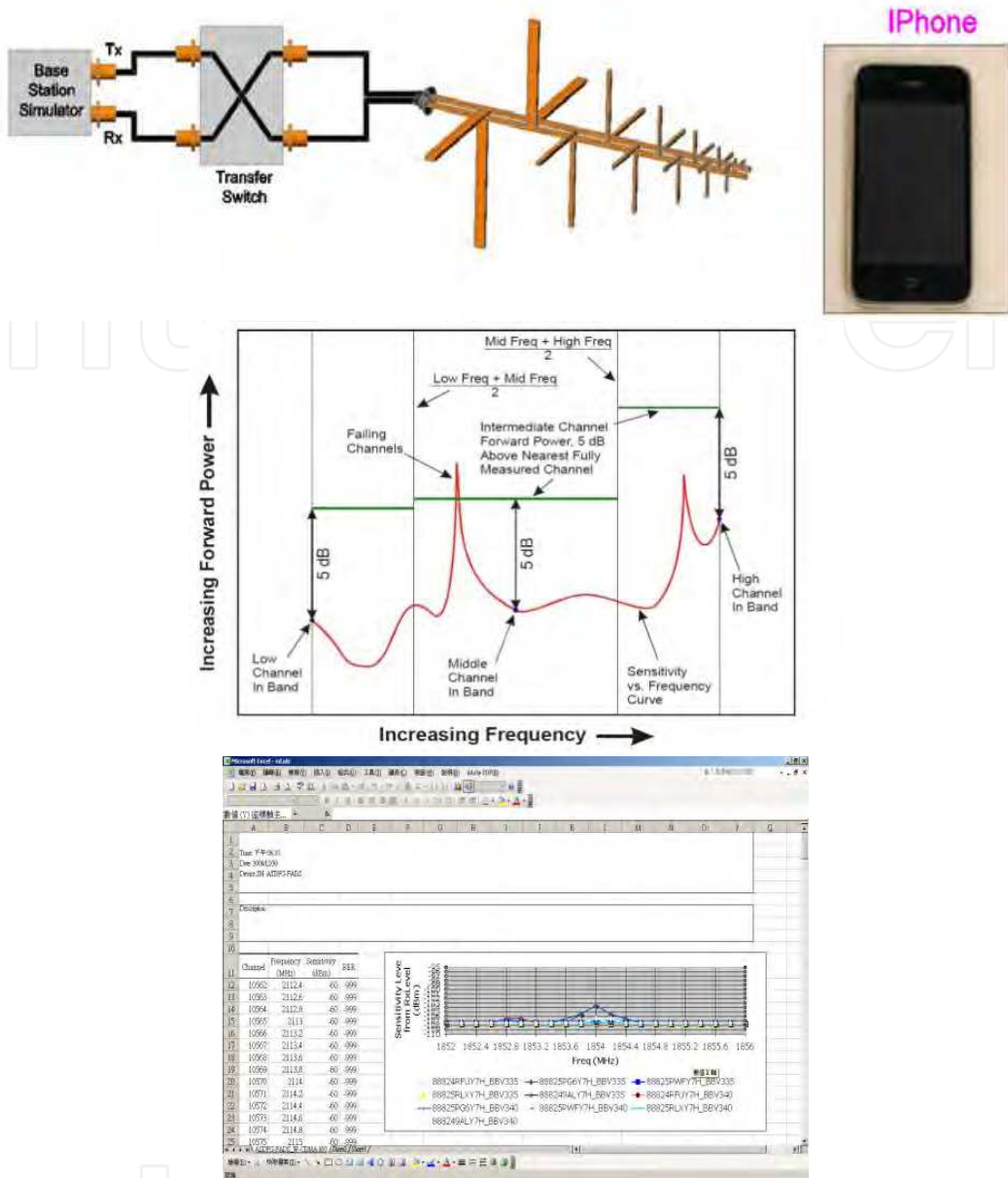


Fig. 8. Alternative way for testing relative sensitivity of intermediate channels.

2.2 De-Sense effect

DeSense is the term representing the noise impact degree on receiver sensitivity. This section will address on the popular TP and camera module about their roles on interference with embedded antenna and discuss the De-sense effect from platform noise coupling.

Nowadays, Touch Panel (TP) and camera module both occupy large part on the smartphone, Tablet PC or NB. Hence no matter where the embedded antennas are placed, the noise emitted from TP and Camera will couple to antenna and thus result in DeSense (Degradation of Sensitivity) problem. On the other hand, all the RF power transmitted by embedded antennas of the wireless products will also couple to nearby TP and camera modules. Those proximate electric (E) and magnetic (H) field coupling will affect normal operation of TP and camera modules.

Figure 9 shows the antenna locations under investigation. In addition, Figure 10 shows the Path-Loss measurement setup and test procedures as following[4]:

1. Put EUT into shielding box.
2. Connect VNA port1 to Tx antenna and laptop antenna to port 2
3. Measure for specific frequencies antenna efficiency of Tx antenna and Rx antenna

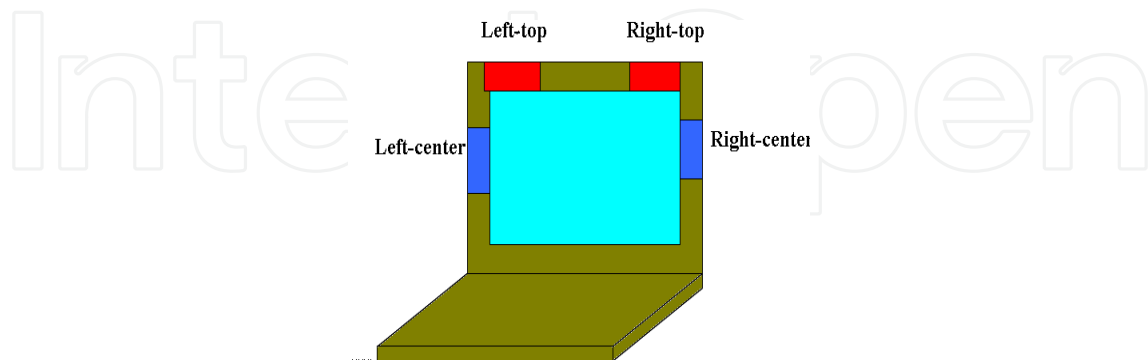


Fig. 9. Antenna locations on laptop display.

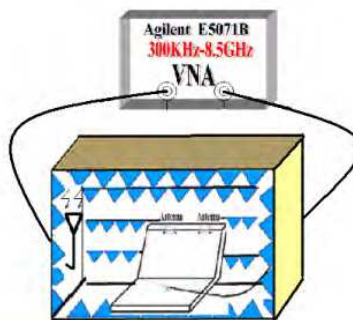


Fig. 10. Test setup to measure Path-Loss.

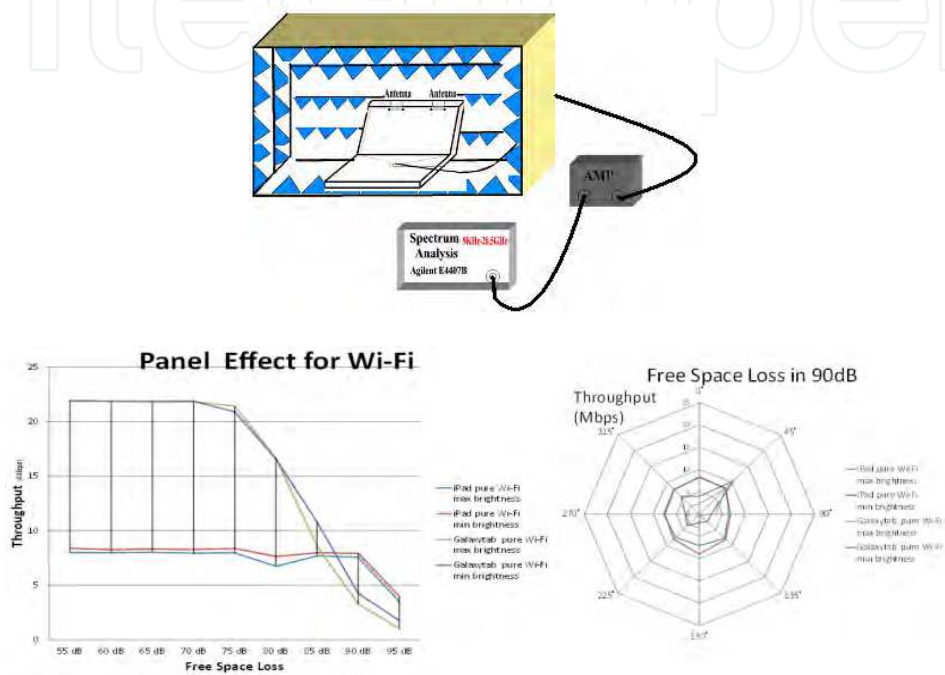
2.2.1 Impact of LCD EMI analysis on 802.11g throughput[5]

In a laptop, there are many interference sources which can be in the form of radiation or conduction. LCD noise is the major interference to the wireless performance. Figure 11 shows the frequency domain measurement setup and measured results for platform noise from LCD. The measurement setup is shown in Figure 11a and the test procedures are described as following:

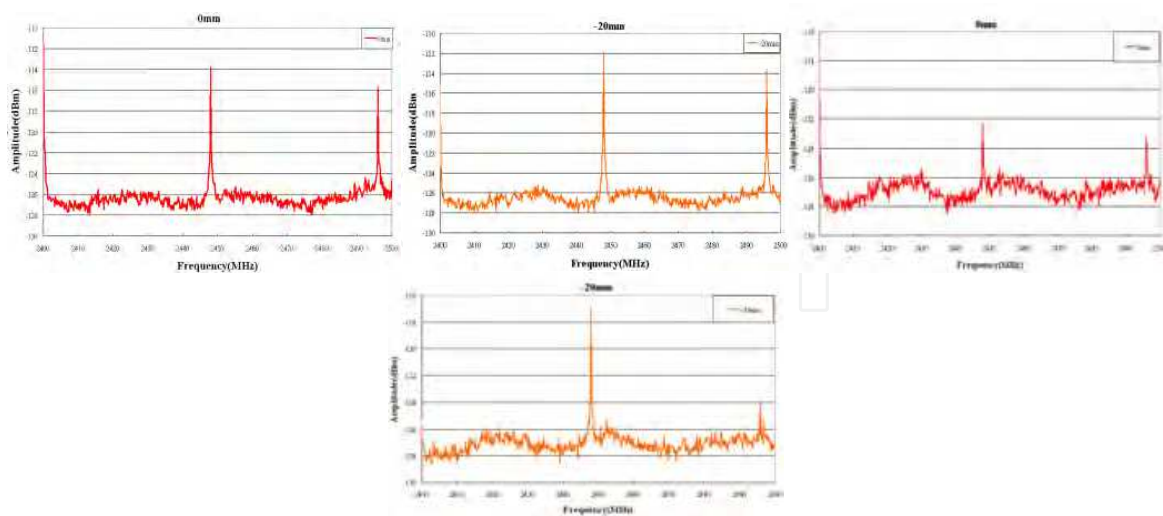
1. Put EUT into shielding box.
2. Connect antenna cable to AMP/Spectrum analyzer via coaxial cable.
3. Power on EUT.
4. Measure noise level for the chosen target frequency.

Figure 11b shows the different antenna placements along the horizontal edge on top of a LCD panel. The measured results show that the noises at 2.400GHz, 2.450GHz, 2.490GHz (harmonics of the pixel clock) are major interference sources that fall into WLAN band. We can obtain 2-5dB noise suppression by simply moving the antenna several millimeters away from its initial location. The comparison for different antenna measurements at different locations shows that the LCD noise might have a significant impact on desensitization to

802.11g. The measurement of antenna positioned towards the left 20mm serves as a reference to quantify the impact of antenna placement on the platform noise measurement. The noise picked up by antennas would desensitizes the receiver and reduced the throughput. Meanwhile, the throughput test procedure and test setup are as follows: the setup consists of an AP (access point), EUT (laptop) and Chariot console throughput software. The AP (access point) and EUT (laptop) are connected through path-loss attenuators to control RFI strength, and the communication traffic is controlled and monitored by a desktop using Ixia Chariot® software as shown in Figure 12a. The system



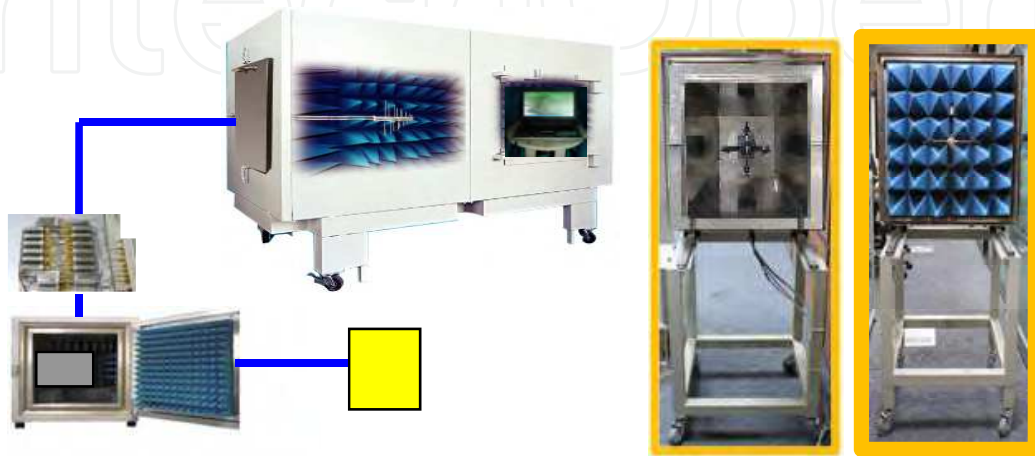
(a) Platform noise measurement setup for antenna port



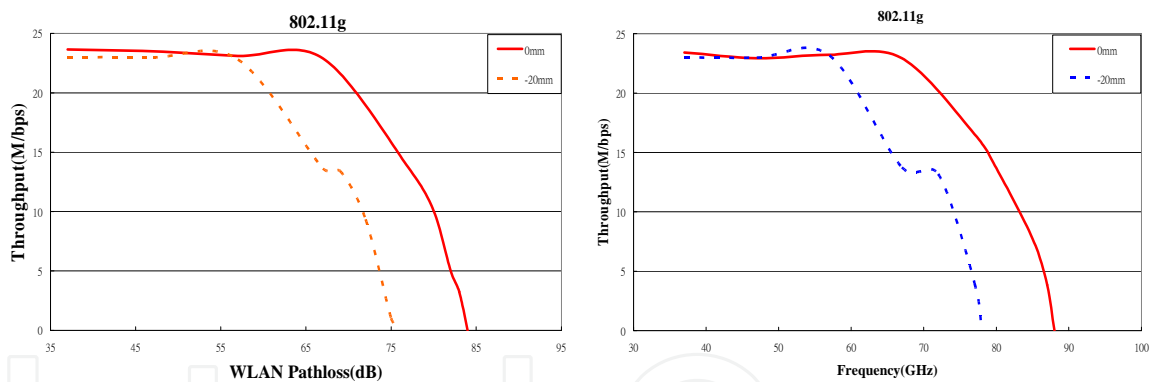
(b) Comparison of the different antennas measurement at different locations on the LCD panel.

Fig. 11. LCD noise measured at antenna port in WLAN band.

path-loss includes cable loss, space loss and attenuators. The results in Figure 12b the real line and dotted line, clearly show that the sensitivity and the throughput decrease as the LCD interference is injected to the communication link between the AP and NIC card. It is found that there is about 10dB desensitization between the two throughput measurements for different locations. It is show that when the LCD noise increases the sensitivity is reduced and performance is also degraded. Moreover, it is again shown that the location of antenna placement is significant to wireless communication performance. Figure 12c shows the photograph of the antenna integrated into a laptop for investigation.



(a) The throughput test procedure and test setup



(b) Throughput comparison for in 802.11g antenna 2 and antenna 3 at two different positions.



(c) Photograph of the antenna integrate into a laptop.

Fig. 12. Throughput comparison in 802.11g for different locations on the LCD panel.

2.2.2 Platform noise analysis of Netbook system[6]

Platform noise analysis can be conducted through the noise floor measurement at antenna port of wireless device. The complete setup for noise floor measurement should at least consist of following hardware instruments: Shielded box, pre-amplifier, spectrum analyser or EMI receiver, high quality coaxial cable, and Netbook EUT.

The frequency-domain noise floor measurement setup for Netbook platform is shown as Figure 11(a). The measuring procedure is as following: Put the EUT Netbook inside the shielded box and connect its antenna port to the pre-amplifier and spectrum analyser. We first measured the ambient noise with Netbook power-off, then powered on the Netbook and measured the noise level within the selected communications bands as interfering platform noise.

Figure 13 shows the noise level captured by the integral WWAN antenna of the Netbook on GSM 850, GSM 900, and DCS 1800 bands. The platform noises on GSM 850, GSM 900, and DCS 1800 bands are shown in Figure 2(a), (b), and (c) respectively. Figure 13(a) shows that the major noise spectrum falls on 864 MHz and 888 MHz, corresponding to the 36th and 37th harmonics of the Azalia Sound Card with 24 MHz fundamental driver frequency.

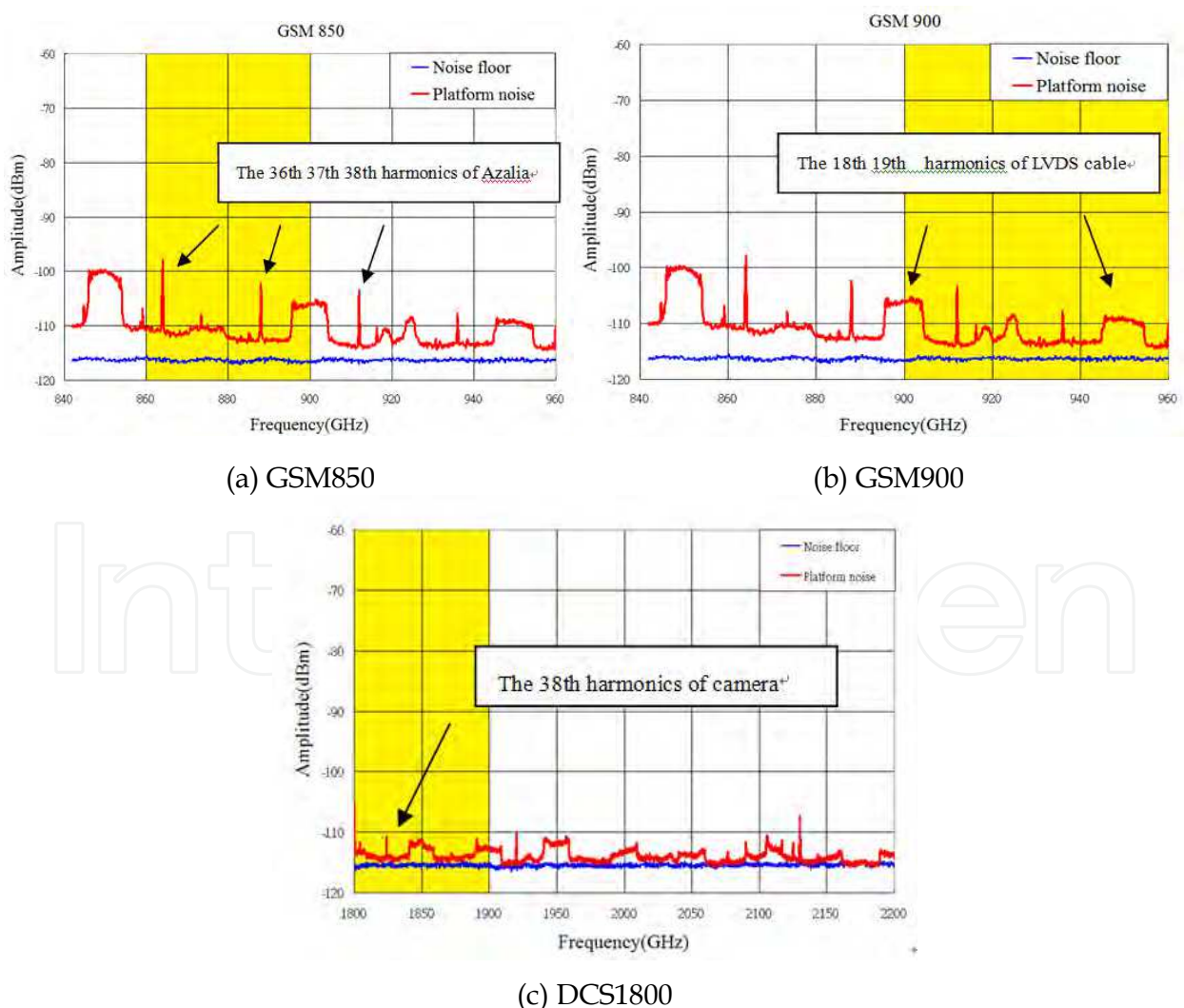
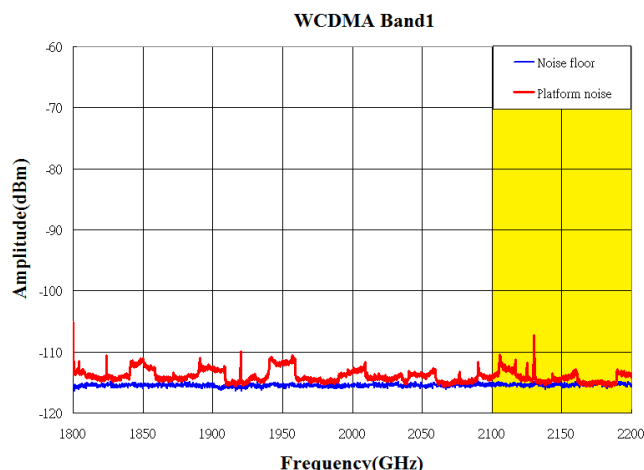


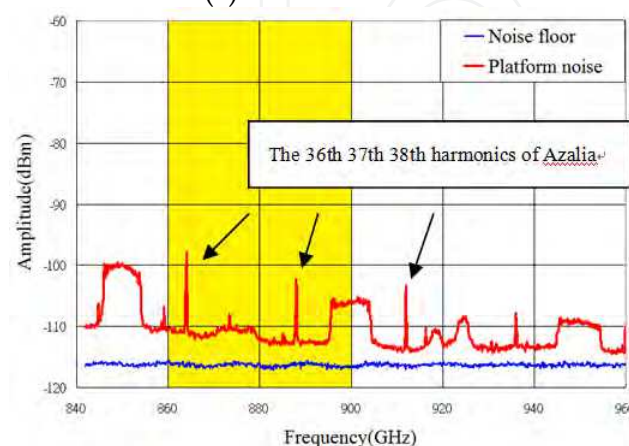
Fig. 13. Measured noise level on WWAN bands of Netbook.

Figure 13(b) shows broadband and regularity characteristics of noise on 900 MHz band. Since the fundamental frequency of the LVDS interconnection cable is 50 MHz and noise spectrum falls between 900 MHz and 950 MHz, we can calculate from system clock map that the noise spectrum received by antenna was originated from 18th and 19th harmonics of LVDS cable. Figure 13(c) shows that the noise measured on DCS 1800 band falls on 1824 MHz, which is 38th harmonic of CCD camera. Figure 13(c) also shows noise occurring around 1850 MHz and 1900 MHz, which are the 38th and 39th harmonics of LVDS cable respectively. From the noise spectrum analysis, we found out that the noise sources mentioned above cause in-band interference on operation bands of GSM 850/950 and DCS 1800 systems frequently. Figure 14(a) shows the noise measurement result on Band-1 of WCDMA, and it appears as lower level and ambiguous. However, because Band 5 of WCDMA almost operate on the same frequencies with GSM 850, it thus suffers interference from the 36th and 37th harmonics of the Azalia Sound Card.

From the platform noise measurement method and clock map analysis, we are able to establish the system design rule for related position and orientation of noise source(s) and antenna(s) placement to suppress in-band interference. We can also utilize various isolation or shielding techniques to effectively prevent the antenna port noise level from platform noise sources, and further reduce the delay time caused by lengthy product debug and speed up testing time.



(a) WCDMA Band1



(b) WCDMA Band5

Fig. 14. Measured noise level on WCDMA bands of Netbook.

2.2.3 Impact analysis of platform noise on TIS of GSM/WCDMA systems[6]

TIS is a figure of merit for receiving performance of a mobile or wireless terminal device. Receiver performance is considered as important to over all system performance as is Transmitter performance. The downlink, or subscriber unit receive path is integral to the quality of the device's operation. The receiver performance of the Equipment Under Test (EUT) is measured utilizing Bit Error Rate (BER) or Frame Errasure Rate (FER). This test specification uses the appropriate digital error rate (as measured by the subscriber unit) to evaluate effective radiated receiver sensitivity at each spatial measurement location. All of the measured sensitivity values for each EUT test condition will be integrated to give a single figure of merit referred to as Total Isotropic Sensitivity (TIS). The BER specification of CTIA on GSM and WCDMA systems for optimal transmitted data rate are 2.44% and 1.22% respectively. TIS measurement not only measures the performance of stand-alone antenna, but also takes wireless device itself into account to realize the practical implementation. We evaluated the EIS (Effective Isotropic Sensitivity) by measuring the minimum received power that met the BER requirement on the test position. The TIS result is able to clearly show the 3-dimensional receiving performance of wireless communications device under specific mobile communications environment.

The complete setup for TIS measurement should at least consist of following hardware instruments: fully anechoic chamber, measuring antenna(s), base-station communications emulator, RF relay switch, high quality coaxial cable, control PC, and position controller. The practical setup for TIS measurement is shown as Figure 4. The operation principle of Figure 15 is as following: Connect control PC to the base-station communications emulator and then make the base-station emulator send test signal to transmit antenna. The power level of transmit antenna is set to -60 dBm for TIS measurement. The power level decreasing step specified by CTIA is 0.5 dB for transmit antenna to measure the minimum power level obtained by receiving antenna. When the transmitted power has been attenuated to some lower level and signal received from receiving antenna to base-station emulator with BER worse than 2.44% (GSM)/1.22% (WCDMA), then we have the minimum receiving power for Netbook.

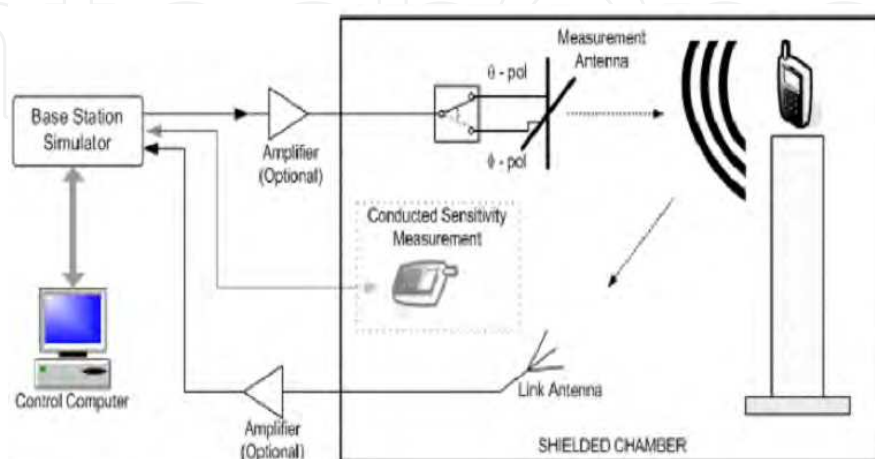


Fig. 15. Setup for TIS measurement.

The results of TIS measurement are shown in Table 1 and 2. The High/Mid/Low channels of GSM850/900 and DCS1800 systems are selected to analyse the platform noise level impact on TIS measurement as shown in Table 1. We found that TIS performance is getting worse as in-band noise increases. Table 1(c) shows the relationship between platform noise level and TIS on CH 512 and CH 698 of DCS 1800 system, it indicates that TIS has 5dB degradation as platform noise increases 2 dB. Table 2 shows the TIS measurement result of WCDMA of Netbook. From the platform noise level and TIS comparison between CH 4357 and CH 4408 of WCDMA Band-5, we found that TIS has 2dB degradation as platform noise increases 1.5 dB. From the observation above, we briefly conclude that TIS performance of the wireless product degrades 2 dB whenever intra-system platform noise level increases 1 dB. It therefore shows that the platform noise is the major factor affecting the receiving sensitivity of wireless devices.

GSM 850	TIS (dBm)	NFS (dBm)
CH128(869.2MHz)	-100.73	-111.39
CH190(882.6MHz)	-102.73	-112.17
CH251(893.8MHz)	-101.19	-112.63

(a) GSM850

GSM 900	TIS (dBm)	NFS (dBm)
CH975(925.2MHz)	-100.74	-108.97
CH037(942.2MHz)	-101.43	-113.18
CH124(959.8MHz)	-100.08	-113.72

(b) GSM900

DCS 1800	TIS (dBm)	NFS (dBm)
CH512 (1805.2MHz)	-103.76	-113.48
CH698 (1842.4MHz)	-98.91	-111.49
CH885 (1879.8MHz)	-102.49	-114.51

(c) DCS1800

Table 1. Measured TIS on WWAN bands of Netbook (a) GSM850 (b)GSM900(c)DCS1800.

WCDMA 1	TIS (dBm)	NFS (dBm)
CH10562 (2112.4MHz)	-105.44	-114.74
CH10700 (2140MHz)	-103.74	-113.12
CH10838 (2167.6MHz)	-106.32	-115.03

(a) WCDMA Band1

WCDMA 5	TIS (dBm)	NFS (dBm)
CH4357 (871.4MHz)	-102.37	-110.63
CH4408 (881.6MHz)	-104.26	-112.17
CH4458 (891.6MHz)	-104.24	-112.56

(b) WCDMA Band5

Table 2. Measured TIS on WCDMA bands of Netbook.

3. RF coexistence problems on product performance [7]

Due to the increasing add-on functions demand for consumer electronics, currently multi-radios, such as WLAN, WWAN, GPS, Bluetooth, and even DVB-H modules, have all been crowdedly embedded and highly integrated in a tiny space of wireless communications platform. Therefore the wireless devices usually have been equipped with more than one antennas, the purpose is to fit for different communication system such as cellular mobile communications, wireless local area networking, and personal area networking. Under this situation, the performance of various kinds of wireless communications is usually degraded by the mutual coupling and interference of closely arranged antennas inside the mobile device. Since the RF modules co-existence has become a critical design problem for wireless communications, we will discuss the RF coexistence problems in this section.

3.1 Isolation required for RF coexistence

Platform noise usually raises the RF receiver noise floor and dramatically degrades system performance by push the E_b/N_0 to the margin when there in-band or out-of-band interference exists. A frequent cause of poor sensitivity on a single channel, or a small number of channels, is due to receiver's in-band noise from broadband digital noise or spurious signals from other coexistent transmitters. We describe in this section the potential coexistence problem for multimode and multiband RF modules, and also illustrate below in Figure 16 the example of isolation required for various RF systems to achieve better service.

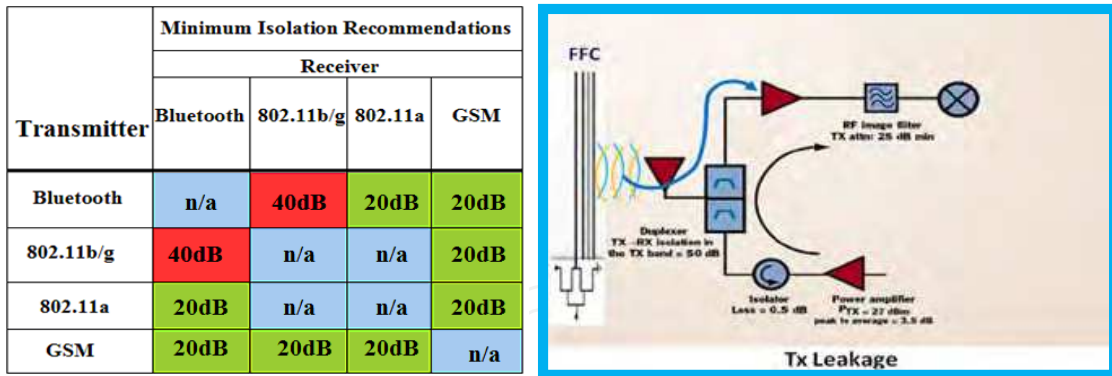


Fig. 16. Tx leakage in FDD system and isolation budget.

3.2 External modulation problem

Even the low-speed digital I/O traces or cables in TP may induce GFSK modulation current, when they are nearby Bluetooth module operating at 2.4GHz. The non-linear ON/OFF switching of digital signal would also play a role as pulse modulation and generate magnetic field through those traces or cables to interfere the DCS and PCS systems. Some extreme case would also happen to WCDMA. The external modulation phenomenon can't be measured by network analyzer until the TP is activated as shown in Figure 17. We also illustrate in this section how the external modulation effect could be found in the final design stage of product with WWAN and BT RF modules ready, however the re-design is needed when platform and TP operate in their normal mode.

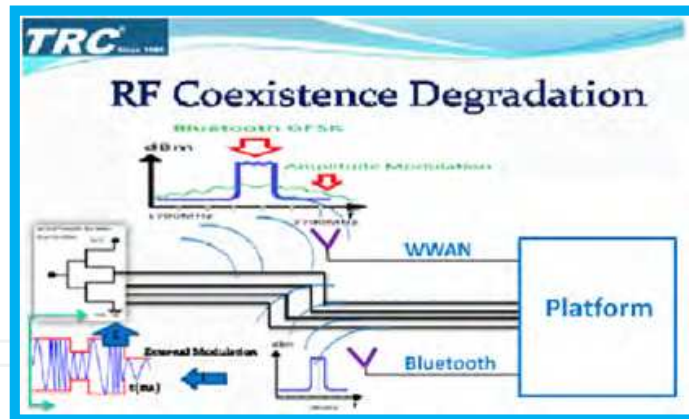


Fig. 17. External Modulation Effect.

4. Platform noise coupling mechanism

The interfering noise sources mentioned above may introduce adverse noise to the nearby wireless modules via conduction or radiation coupling or even both. The digital noise coupled from broadband digital or narrow-band RF devices may result in in-band interference and further degrade the performance of wireless communications, and vice versa. Since the digital noise would cover a wide range of frequency, we will illustrate in Figure 18 and 19 the three potential coupling mechanisms between the noise sources and victim circuit or module: conducted coupling, crosstalk coupling, and radiated coupling.

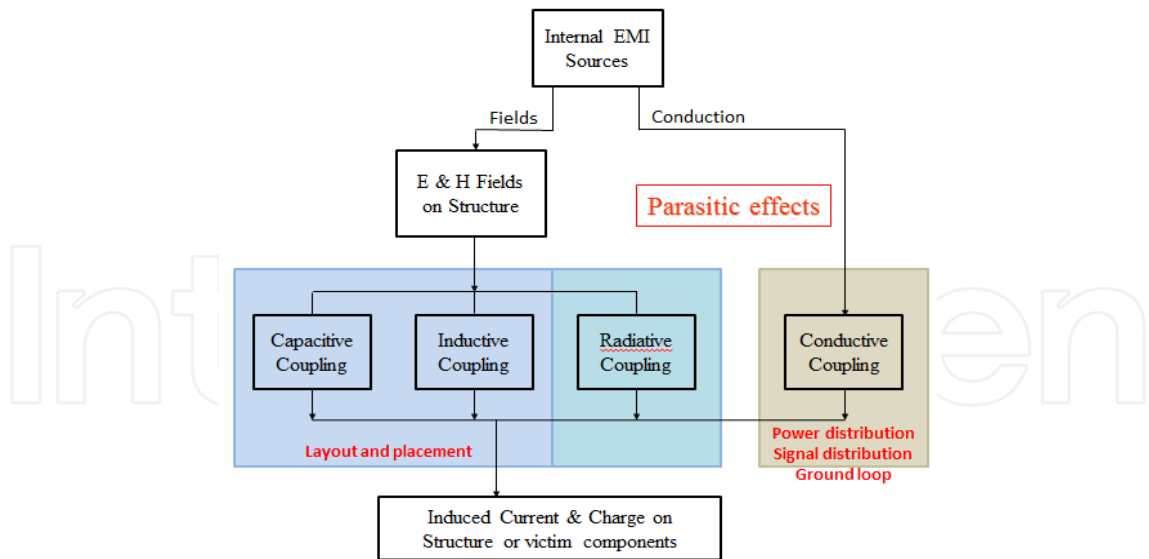


Fig. 18. Different coupling mechanisms.

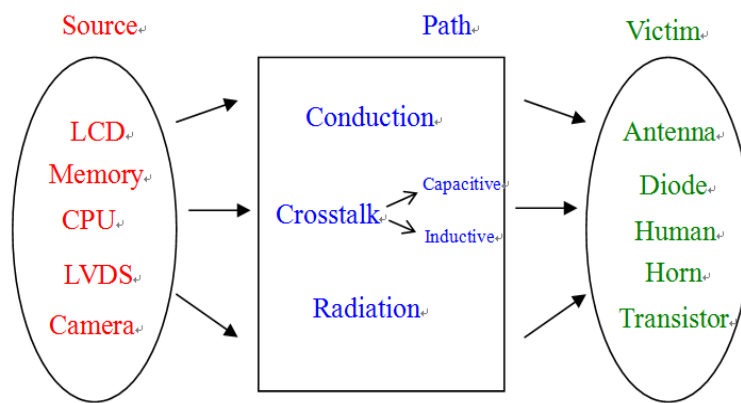


Fig. 19. Illustration of possible noise coupling for wireless device.

The Figure 20 illustrates the EM interaction between TP and embedded antenna, and the photograph of Figure 21 shows the DCS1800 and PCS 1900 transmitted power coupled to LCD panel.

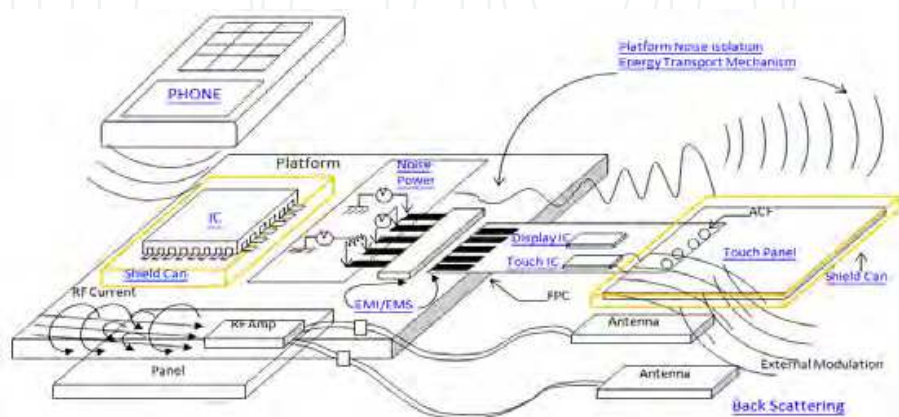


Fig. 20. EM interaction between TP and embedded antenna.

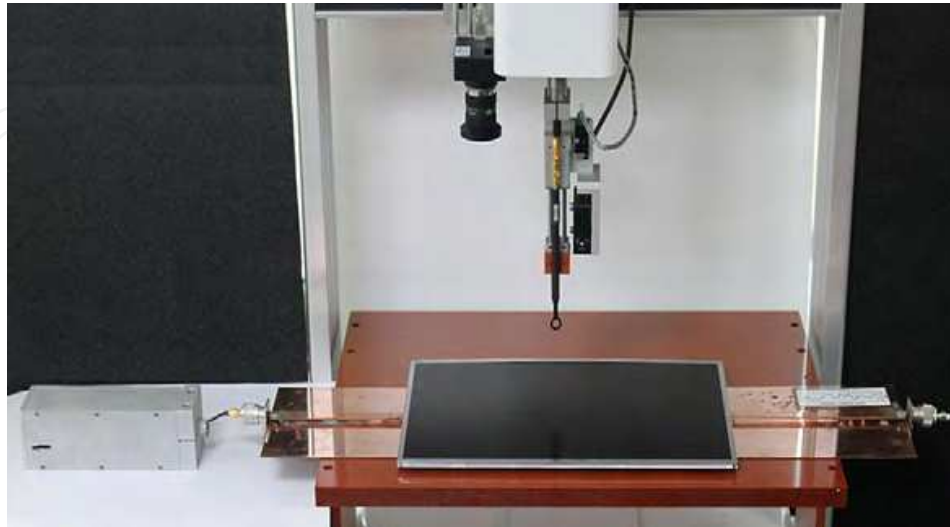


Fig. 21. Illustration of DCS1800 and PCS 1900 coupling to LCD panel.

4.1 Analysis of conductive coupling

The first step of the degradation of sensitivity (De-sense) measurement is conducted testing, because understanding how the interference platform noise conducted to the RF receiver is the most important issue for further analysis. Even the same probability distribution function of noise, there is possible to cause different De-Sense impact depending on the receiver implementation.

The best way to obtain the conducted De-Sense effect is to use the internal WWAN module or chip set of mobile device for RSSI measurement as shown later in Figure 25. The left figure shows a 50 ohm terminated at antenna connector to read the WWAN RSSI data. The figure in the center shows the dummy WWAN module with circuit ground and chassis ground, and the WWAN card inside the shielded box is connect to the dummy WWAN card via coaxial cable to read the RSSI data again. The right figure shows the dummy WWAN module with chassis ground and WWAN card to read the RSSI data. The RSSI data read from the same RF receiver with three different conditions described above will help engineers easily identify the platform noise.

4.2 Analysis of near-field coupling from antenna to embedded devices

Since the antenna is usually implemented in the proximity of TP and camera, the near-field coupling to the nearby TP and camera would sometimes result in malfunction due to the transmitted power (Figure 21). The electromagnetic field distribution on TP due to antennaradiation is shown in Figure 22 below.

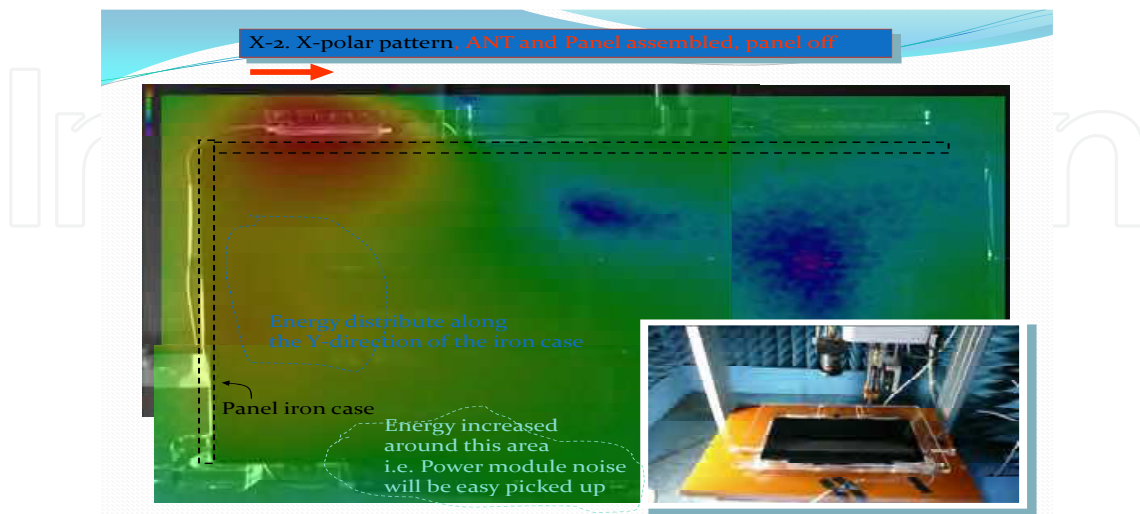


Fig. 22. Antenna radiation coupling.

4.3 Resonance issues of mechanic structure

The LCD panel of Notebook and the enclosure or PCB would usually create a resonant structure. The related resonance issue could be explained with the following measuring methodology.

1. Connect port 1 of network analyzer to LVDS cable and WEB camera cable via a coupling fixture (Balun and low-mu ferrite core as absorbing clamp) for energy transferring to the LVDS cable.
2. Connect port 2 of network analyzer to the embedded antenna of Notebook via its own mini-coaxial cable.
3. Measure the VSWR of port 1 and port 2 respectively. Both VSWR must be less than 2.5 to ensure the testing setup is good enough for efficient energy transfer.

When enclosure of LCD panel was removed, the maximal difference of S_{21} mentioned above can reach upto 20dB. Hence we can conclude that LVDS and Web camera cables, embedded antenna and its mini-coaxial cable, LCD panel all will lead to amplification of coupling between the interference sources and receiving module.

5. Platform noise measurement techniques

Conductive or near-field coupling platform noise will raise the level of RF receiver noise floor and thus cause performance degradation, and thus we need to investigate the isolation required as shown in Figure 23. We will describe the related measurement techniques in this section.



Fig. 23. Platform noise coupling.

5.1 Noise level measurement

The result of noise level measurement represents the de-sense degree caused by IC, component, module, power circuits, PCB layout, interconnect wires, connector, and even the mechanical construction of the product. This section will describe the different methodology for the measuring procedures.

5.1.1 System noise measured with spectrum analyzer

- Measured by frequency domain sweep for multi-bands (GSM 850, 900, PCS1800 etc.) as shown in Figure 24.
- The Noise Distribution Function at area A is close to Gaussian distribution (Maximum Hold - Average = 10dB) , area B is close to CW (little amplitude variation with time)
- Noise limit level means the probability density function (PDF) of noise power is equivalent to Gaussian. Limit line for area A applies for the calculation described above, but PDF correlation is needed for area B.

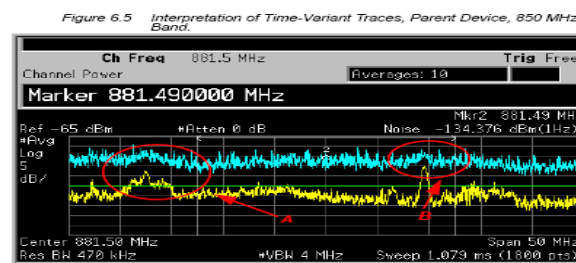


Fig. 24. System noise measured with spectrum analyzer.

5.1.2 System noise measured with WWAN card

In practice, it is more reasonable to measure system noise with a WWAN card because the RSSI is ready to appear at I/Q demodulator output, since it is the same sampling clock and module size for WWAN communication. The noise power measured from RSSI of WWAN add-on card can therefore in compliance with the definition of N0. The testing configuration and measurement are both shown in Figure 25.

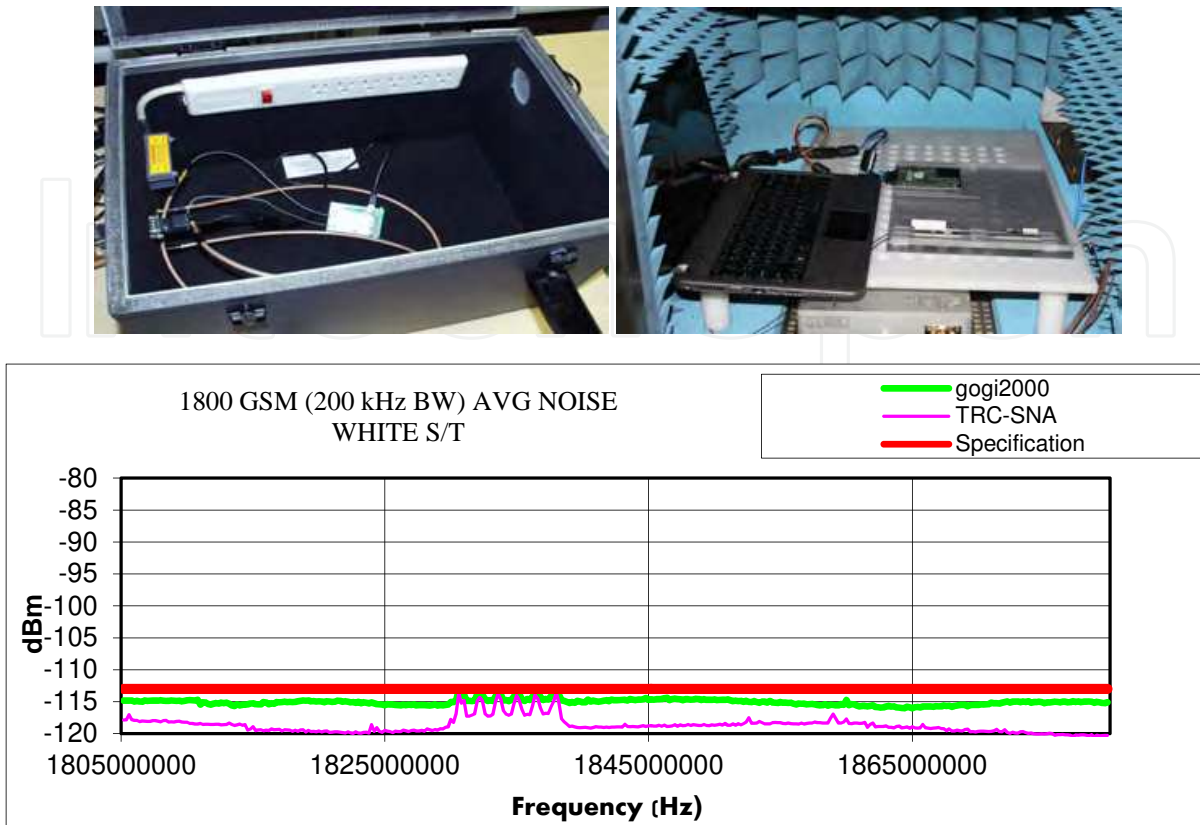


Fig. 25. Test configuration and system noise measured with WWAN card.

The SNA option shown in Figure 26 can also provide the De-Sense Measurement function. The software provides the Base-Station simulator, and provides VSG for WWAN and GPS measurement. The hardware provides switch and combiner for testing signal condition selection.

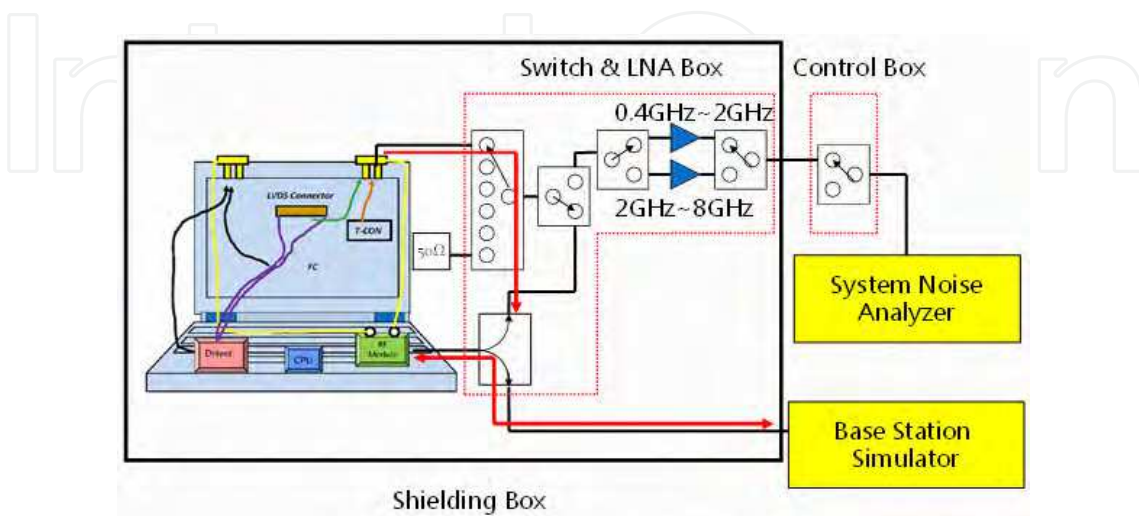


Fig. 26. The SNA test configuration.

The benefit and applications of SNA can be listed as following:

- Provide measurement adapter for fixing the antenna cable routing inside NB and Tablet PC.
- Provide testing fixture for different size LCD display panel.
- Provide testing fixture for SSD noise budget measurement
- Provide measurement adapter for ground isolation between smart phone and SNA (two Balun back-to-Back in series)
- Provide debugging plot to view each band at the same time.

5.1.3 SNA calibration at limit level

Since the WWAN or LTE cards are not originally designed for the noise measurement, and these cards need to provide about 60dB dynamic range for receiver. Therefore the variable-gain amplifier must be utilized for AGC purpose at the same time when the noise floor of receiver reaches up to 6dB. SNA is here designed to measure the platform noise. The dynamic range of receiver is from 4dB under limit line level up to 16dB above limit line level. With front end LNA implemented, the noise floor of SNA system is around 2dB and the average noise floor level is 4dB lower than that of WWAN or LTE card.

The noise floor level for WWAN is -115dBm. However, the limit line level for some particular applications like identifying the main noise source (system noise or panel noise) will be -114dBm. We can use the receiver with -115dBm noise floor level to receive the noise with level of -114dBm, and there is 1dB uncertainty for signal to noise level result. Since the average noise floor level can be obtained for SNA is -119dBm, it can provide more accurate signal to noise ratio for -114dBm measurement in general cases as in Figure 27.

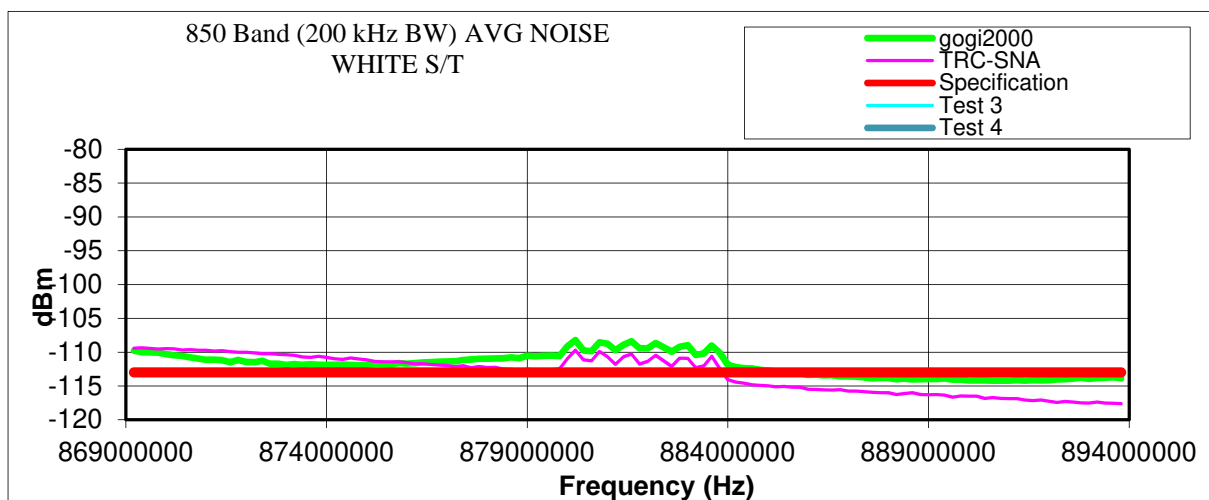


Fig. 27. Noise floor level obtained for SNA.

5.2 Throughput measurement

The throughput standard is widely adopted in different applications like video stream, online game, video conference. For example, you may need 1Mbps or more for YouTube HD video. Throughput is the most common for user experience regarding wireless RF

performance, therefore throughput test need to consider how the user interacts with the RF device. For example, 90dB path loss for laptop 802.11g WLAN may represent that AP is 200 meters away in the free space environment, however the hand and head may cause the range for 90dB path loss much less than 20 meters for smart phone VOIP application. Some real-life products throughput test result has been illustrated in Figure 12 and the Root Cause Analysis (RCA) procedure will be addressed later in section 6.

5.3 Antenna surface current and near-field surface scanning

The current distribution on antenna surface represents the different sensitivity on antenna near field boundary, because the physical geometry of antenna will cause different field intensity coupled via the uniform magnetic flux. Antenna surface current also represents the immunity level for TP and Camera. As to digital noisy components, we can utilize the noise level results to locate the noisy components and identify their noise radiation pattern. We can utilize the near-field surface scanning method to observe the surface current distribution of antenna and locate the noise sources for platform noise analysis.

5.4 De-Sense measurement

De-Sense is self-referred to same subjective device operating in different condition and compared the platform noise impact. For example, a GPS module is first performed conducted test in a shielded box and obtains the $C/N=40\text{dB}$ at -138dBm receiving level. While the same module is then bundled in a wireless platform and performed the conducted test again, the receiving level become -130dBm for keeping $C/N=40\text{dB}$. In this example, we found that the conducted platform noise causes GPS module de-sensed by 8dB. When the antenna terminal and GPS signal is fed to GPS receiver through a combiner, we now need -123 dBm to keep $C/N=40\text{dB}$ and thus a 7dB de-sense caused by platform noise picking up from antenna. Furthermore, when the internal device, like Bluetooth, is active or hand-held device resting on desk, the interaction between platform noise and antenna resulting in different de-sense effect can be easily observed in all those test cases. The noise current at different locations can also be represented with the de-sense Data. The methodology and measuring technique illustrated below in Figure 28 can be applied for investigating GPS degradation of sensitivity caused by platform noise.

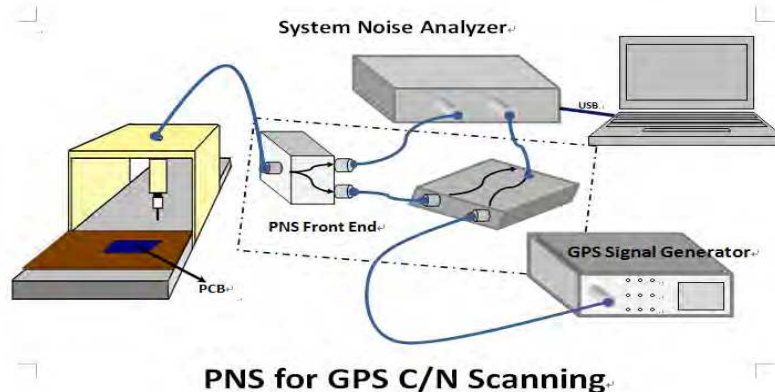


Fig. 28. GPS C/N Scanning.

5.5 Noise measurement at antenna terminal

Since the antennas are the most important port for wireless communications as electromagnetic energy receiving component, they are also susceptible to nearby platform noise. Hence the analysis and measurement of noise level at antenna port is critical for RCA of wireless device to improve link performance. Figures 29-31 show the measurement techniques and configuration for noise measurement at antenna terminal.

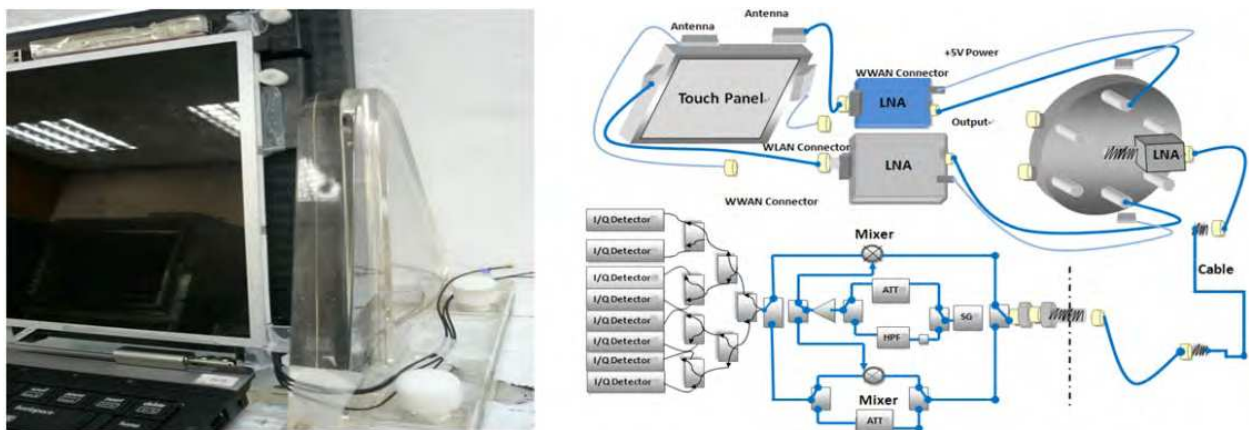


Fig. 29. LCD panel test fixture and the measurement circuits.

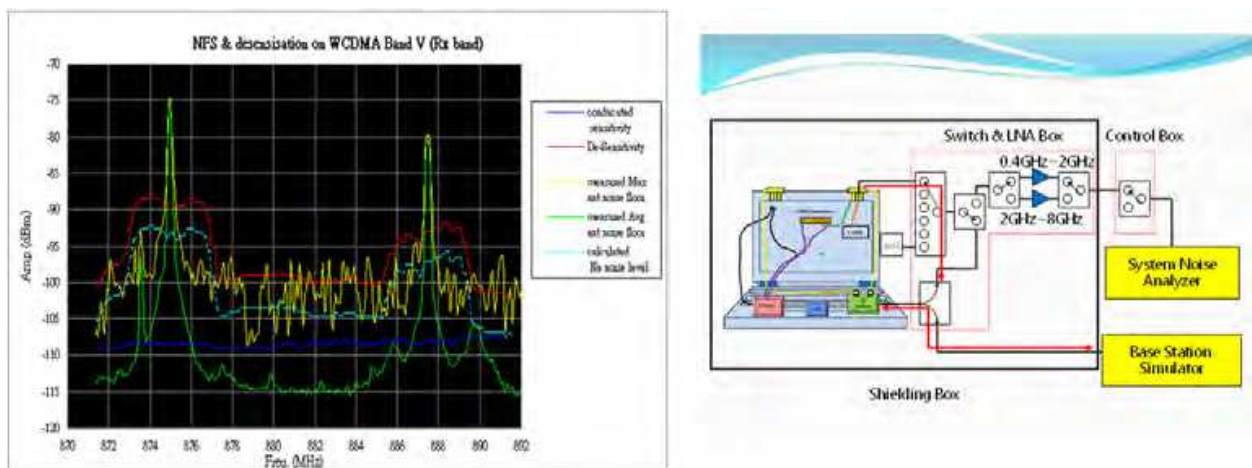


Fig. 30. Platform noise and de-sense measurement at antenna terminal.

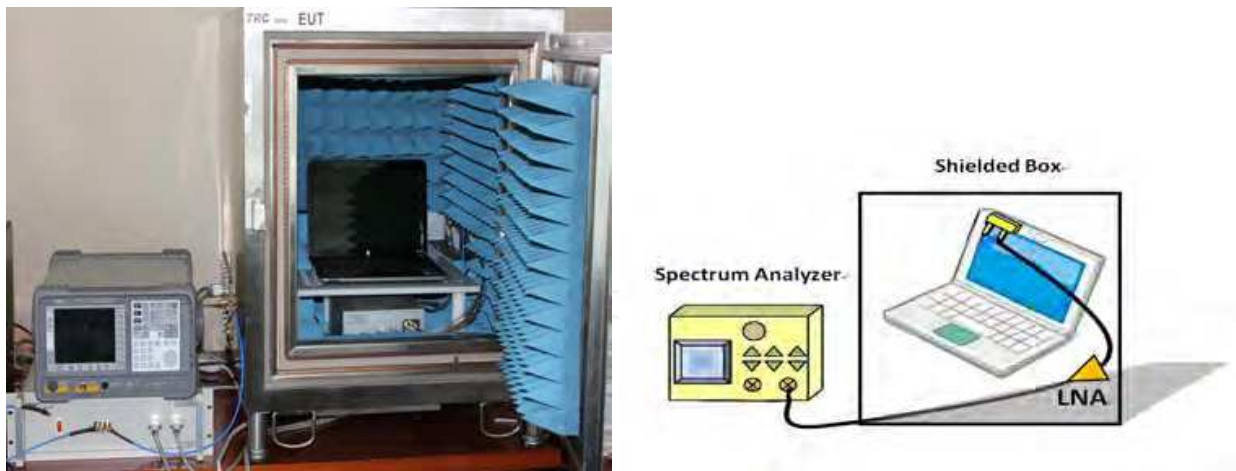


Fig. 31. NFS system and measurement setup.

From the various platform noise measuring techniques described above, we can summarize the comparison as Table 3.

	Measurement Type	Measurement Speed	End to End Calibration	Software User Interface	Correlation
SNA Same LNA and Switch as TRC NFS	Channel	10 times faster than WWAN card	Gaussian Noise Level Cal. At limit line level.	Same as the NFS & Provide the debug mode "View Plot" display test result	Within Limit Line + - 3dB range within 1dB error with WWAN & LTE Card
WWAN Card LTE Card	Channel	Very Slow	N.A .	Depend on Card Vendor of NPT utility	Same WWAN card cab be 2dB error
TRC NFS	Sweep Freq.	Very Faster	LNA & Switch	Well Accepted	Big Difference in Broadband

	Receiver Noise Floor Level	Antenna VSWR Check Before Noise Measurement	Test Fixture, Test Kit and Measurement adapter	De-Sense versus Platform Noise Plot
SNA	Average At 200KHz Channel -119dBm	SNA provide the option for the internal VSWR bridge, Each time debug and close the enclosure should be check the antenna, ensure the antenna is keep the same as original.	Measure the Adapter Insertion Loss for Correction. LCD Test Fixture Can be integrated with LNA and the antenna protect by dielectric material.	Software support the for different brand of base station simulator and VSG, Measure the De-Sense corresponding to the Noise Level.
WWAN Card LTE Card	Average -115dBm	N.A.	N.A.	N.A.
TRC NFS	Depend on Spectrum.	N.A.	N.A.	N.A.

Table 3. Measurement techniques comparison.

6. Design techniques for platform noise improvement

This section will present the Tablet PC as case study to describe the problem-resolving methodology for throughput degradation.

6.1 Identify the main noise source

The first step to solve the interference problem is to identify the main noise source, and then we can further to implement resolving techniques like filtering, shielding, and re-layout, etc. The procedure can be demonstrated below in Figure 32.

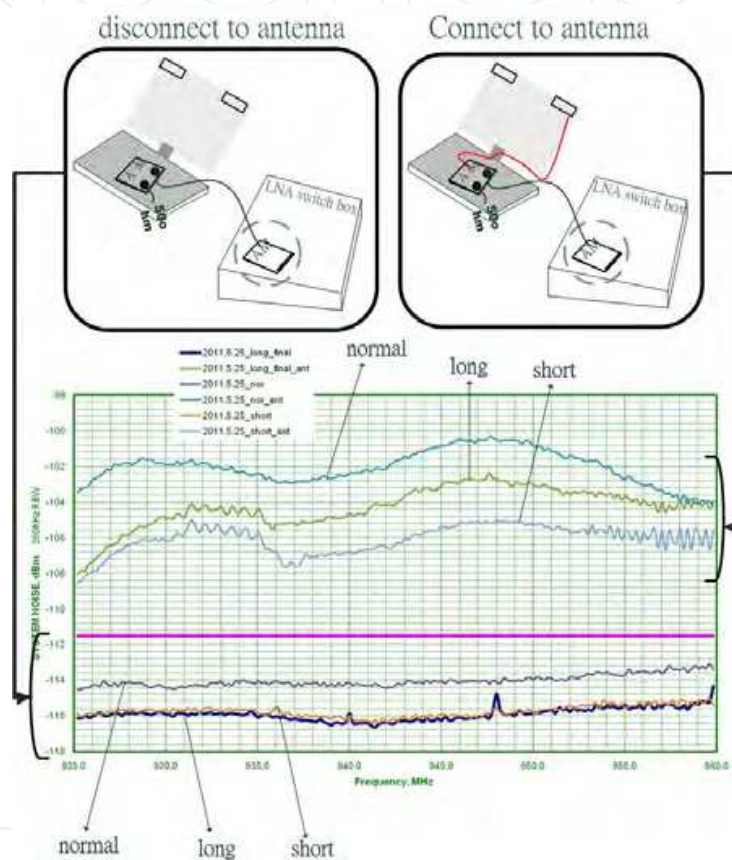


Fig. 32. Use built-in antenna to identify noise source from measured spectrum.

Those engineers who are responsible for resolving noise problem may add the copper foil or put an absorber to cover the IC, routing the antenna cable, re-installing the panel, plugging antenna connector to test port, and they may affect the antenna or noise test results after those activities. Therefore, the antenna VSWR characteristic must be checked before noise measurement. The VSWR measurement of antenna is a quick way to check if the antenna is still kept the same configuration as originally implemented, because 3D radiation pattern and efficiency measurements of antenna usually take 2~3 hours. However, the SNA option described early can provide an embedded VSWR bridge and therefore could automatically check VSWR of each measuring port before noise measurement as shown in Figure 33 for LTE band. There are two kinds of LCD panel testing fixture can be designed for different panel size as shown in Figure 34 and 35.

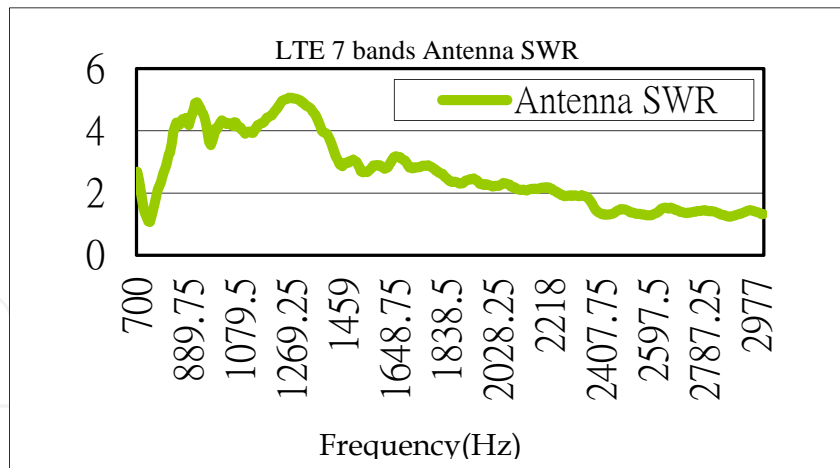


Fig. 33. VSWR of each measuring port before noise measurement for LTE band.

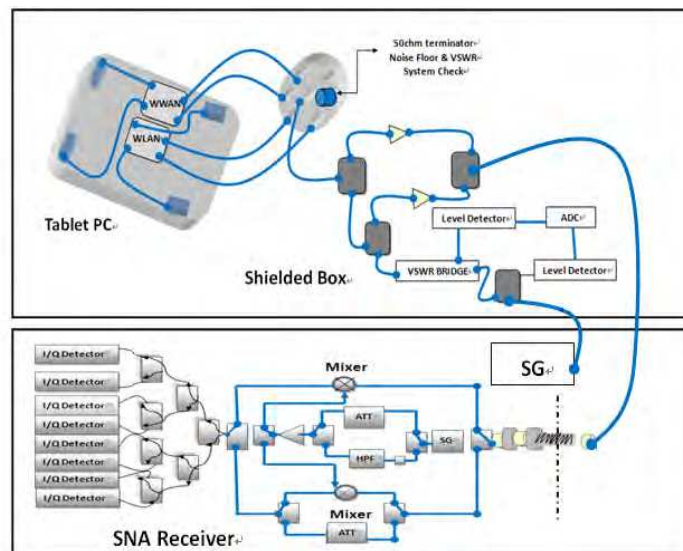


Fig. 34. LCD panel testing fixture integrated with LNA and SNA result for LTE.

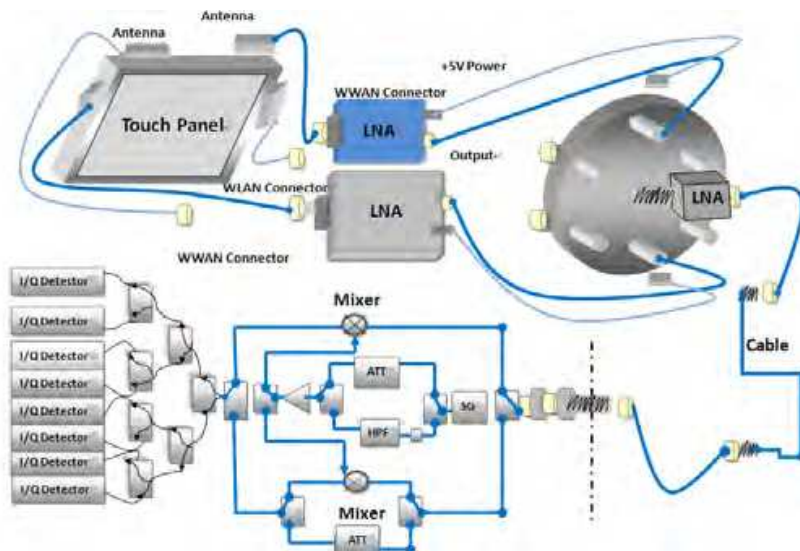


Fig. 35. LCD panel testing fixture with LNA and antenna protected by dielectric material.

6.2 Platform noise isolation

TP and camera are not the only modules resulting in the platform noise problem, but the product's assembly construction such as antenna and its mini-coaxial cable routing, TP and its LVDS cable, camera and its USB cable will also bring up noise problem. We can utilize some design techniques, like component placement and orientation, cable routing, shielding etc. to improve platform noise isolation.

6.3 Antennas isolation [8]

Noise current distribution and antenna surface current are most important message for solving the sensitivity degradation problem. We can use a network analyzer deliver the energy to TP's LVDS or camera's USB lines and measure the insertion loss at antenna port, and that is the most commonly utilized technique to obtain the isolation situation of platform noise.

With the highly integration of powerful computing and multi-radio communications devices in a single product nowadays, multiple antennas are usually implemented to achieve the seamless and convenient communication services. However, the closely placed antennas have resulted in intra-system coupling interference and therefore severely degraded the performance of various kinds of wireless communications. The isolation technique for antenna systems must be implemented to reduce the mutual coupling between coexistent various RF systems. In this section, we will show the optimal isolation achieved from antennas separation, orientation, and utilization of periodic structure to reduce the mutual coupling interference.

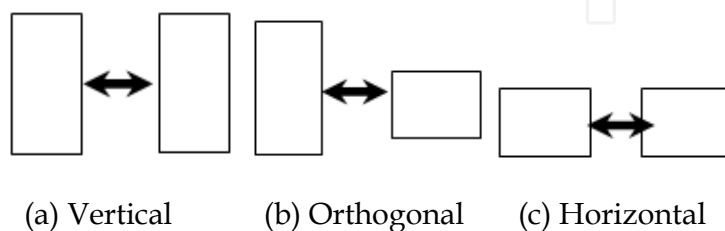
The isolation requirement between coexistent RF systems is shown in Table 4. The placement of two chip antennas under investigation for Bluetooth and 802.11b/g WiFi systems inside the mold notebook computer is shown in Figure 36. The chip antennas are fabricated on FR4 with dimension of 1.6 mm thickness and 35mm × 30mm area, and it is fed by microstrip to achieve 50 Ω impedance-matching. The configurations for different spacing and orientation between coexistent antennas are shown in Figure 37 to analyze the mutual coupling effect.

Transmitter	Minimum Isolation Recommendations			
	Receiver			
	Bluetooth	802.11b/g	802.11a	GSM
Bluetooth	n/a	40dB	20dB	20dB
802.11b/g	40dB	n/a	n/a	20dB
802.11a	20dB	n/a	n/a	20dB
GSM	20dB	20dB	20dB	n/a

Table 4. Isolation requirement between coexistent systems.



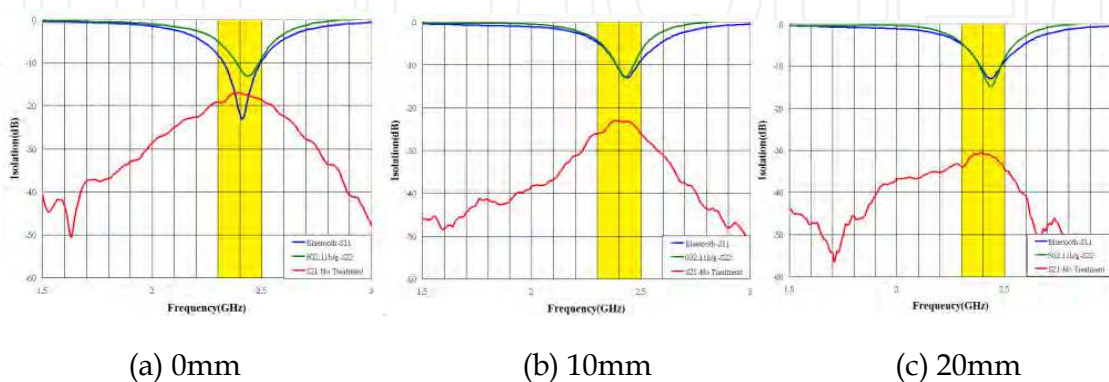
Fig. 36. Placement of two chip antennas inside mold.



(a) Vertical (b) Orthogonal (c) Horizontal

Fig. 37. Three orientation for antennas placement.

The reflection coefficients (S_{11} and S_{22} are reflection coefficients for Bluetooth and 802.11b/g respectively) and isolation (S_{21}) between each other were then measured and shown in Figure 38. The results clearly show that the isolation between antennas is much worse when they are both placed in vertical polarization with main lobes coupling. We then oriented the antennas in orthogonal direction to each other and separated antennas by moving 0mm, 10mm, and 20mm respectively. The measured results of reflection coefficient covering 2.4GHz-2.483GHz in Figure 39 show that the isolation is much better due to orthogonal polarization to each other when they are oriented in orthogonal direction. Finally, we placed both antennas in horizontal direction and adjusted the separation between them, the results in Figure 40 also show better isolation than vertical placement due to main lobes decoupling. Table 5 compares the isolation performance between various orientation and separation for both antennas, and it shows that the orthogonal and horizontal orientations gain almost 6-9dB improvement in isolation except 4 dB difference for 0mm separation.



(a) 0mm

(b) 10mm

(c) 20mm

Fig. 38. Measured results for various antenna spacing with both antennas oriented in vertical direction.

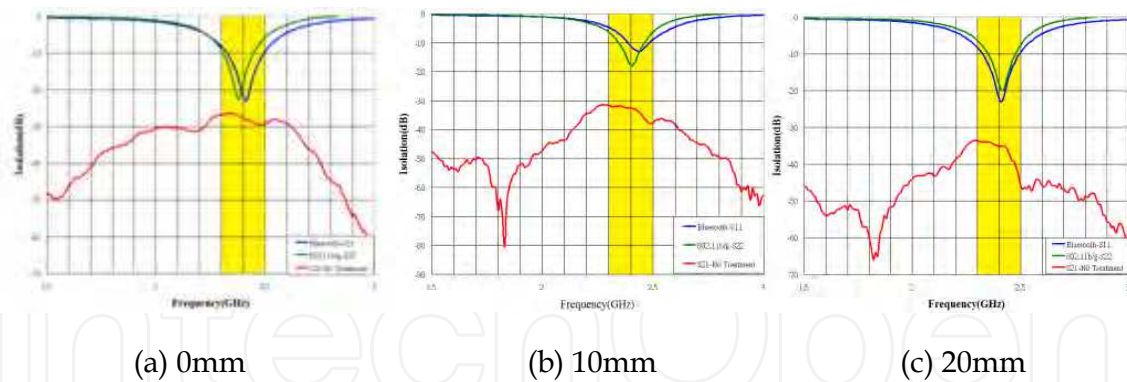


Fig. 39. Measured results for various antenna spacing with both antennas oriented in orthogonal direction.

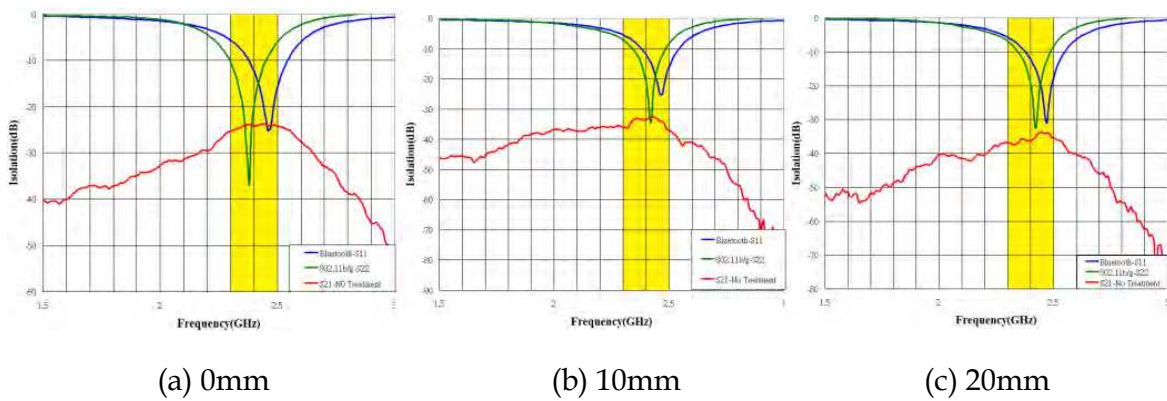


Fig. 40. Measured results for various antenna spacing with both antennas oriented in horizontal direction.

Orientation \ Separation	Vertical	Orthogonal	Horizontal
	Isolation		
0mm	16.9dB	28dB	24.1dB
10mm	23.1dB	32.6dB	33.1dB
20mm	30.8dB	36.2dB	36dB

Table 5. Measured results for various antennas placement configuration.

6.3.1 Suppression of mutual coupling interference between coexistent antennas [8]

The applications of EBG structure in antenna not only could improve gain and radiation efficiency, it could also help suppress side lobes and reduce coupling effect. Since isolation requirement could not be met by orientation and separation arrangement between antennas from the above measurement, we therefore chose the best placement configuration with orthogonal orientation and 20 mm separation for further investigation utilizing EBG

structure. We placed the EBG structure beneath the antennas with 7.5mm (less than $\lambda/4$) and 15mm (about $\lambda/4$) distances as shown in Figure 41 and investigated the mutual coupling characteristics. Figure 42 shows the results with 7.5 mm separation between antennas and EBG structure for various antenna orientations. Because of high impedance surface from EBG structure, the 40 dB isolation requirement between antennas could be achieved and parallel-plate guided wave coupling could also be suppressed. Figure 43 shows the results with 15 mm separation between antennas and EBG structure for various antenna orientations.

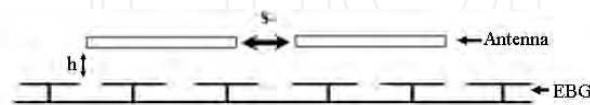


Fig. 41. Configuration of antennas and EBG structure placement.

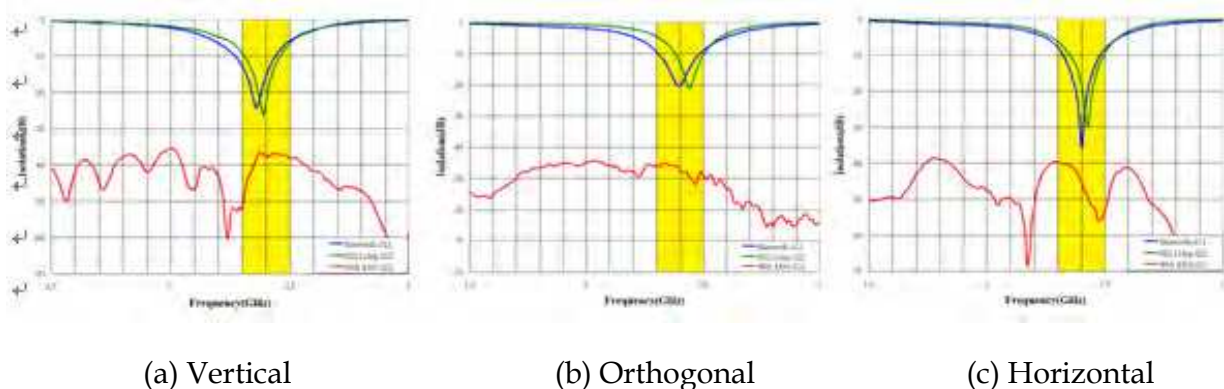


Fig. 42. Isolation and S11 of antennas for various orientation with antennas separation 20mm and EBG-antennas spacing 7.5mm.

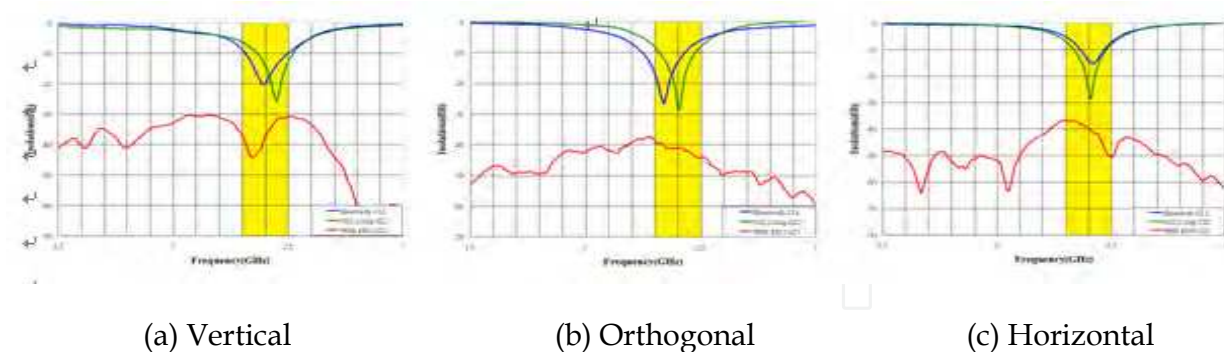


Fig. 43. Isolation and S11 of antennas for various orientation with antennas separation 20mm and EBG-antennas spacing 15mm.

Table 6 compares the isolation performance with and without EBG structure for various antenna orientations, and it shows that 37.7 ~ 48dB and 35.7 ~ 40.9dB isolation between antennas can be achieved with EBG structure placed beneath antennas 7.5mm and 15mm respectively. When EBG structure moves closer to antennas, we can obtain better isolation between antennas.

Orientation \ Separation Between Antennas and EBG	Vertical	Orthogonal	Horizontal
	Without EBG	30.8dB	36.2dB
7.5 mm	37.7dB	48dB	47.4dB
15 mm	35.7dB	40.9dB	40.5dB

Table 6. Comparison of isolation improvement from EBG structure with antennas separation 20mm.

6.4 Keyboard grounding requirements

The large metal plate of a keyboard can act as an integrated shield to prevent noise radiating from the base chassis. However, the mechanical grounding structure needs to be taken serious care of its EMI effect on radio performance, because it is not uncommon that EMI noise radiated from the ground-base to antennas mounted around LCD panel when the keyboard is removed as shown in Figure 44. This means that we are not getting any shield effect from the keyboard, and in fact the keyboard helps EMI ground noise radiating from the base like a large antenna. To make the keyboard a useful shield for all WWAN frequencies, it is necessary to conductively contact ground structure every 1/20th wavelength or so as shown in Figure 45.

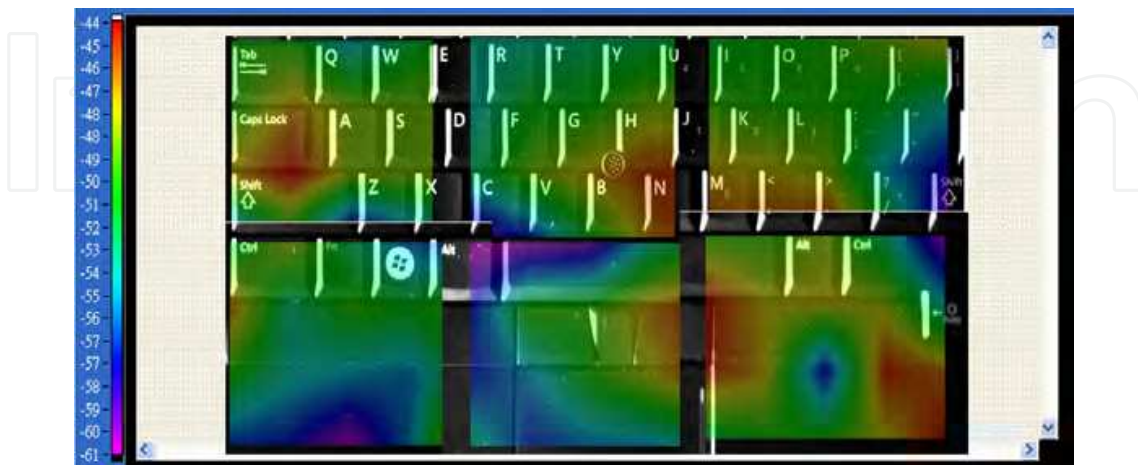


Fig. 44. Field distribution on metal shield of LCD panel and nearby antenna.

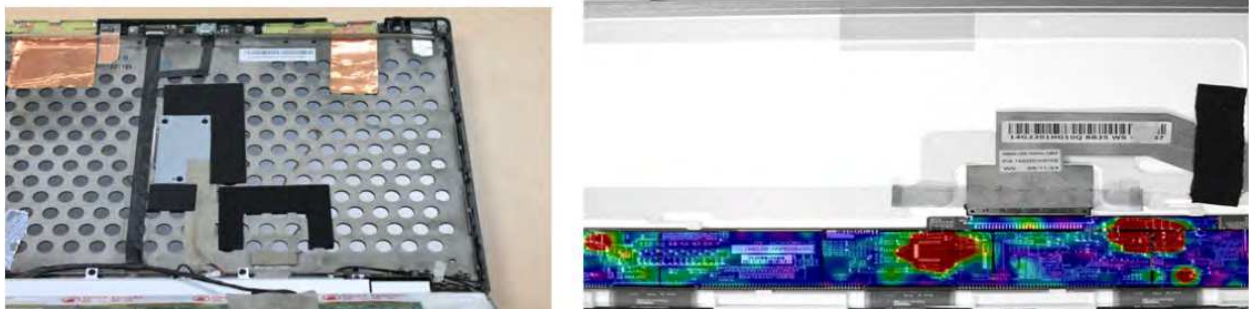


Fig. 45. Metal plate for LCD panel shielding purpose.

Grounding the motherboard to the chassis wherever possible (screw holes, connectors, etc.) will help reduce EMI radiation from the motherboard. The grounding contacts should follow EMC design guidelines for length to width ratio requirement to prevent from adding a radiation structure rather than providing a noise-reduction ground point. Every effort should be made for each screw and contact point of the motherboard to the chassis for a good chassis ground point.

The grounding of the heat sink also raises a problem for ESD, EMI, and platform noise of wireless devices, therefore improvement should be made in the grounding of the heat sink (cooler). The improvement should include: enabling better DC grounding at “spring contact” points, and no non-grounded arms longer than 7mm are allowed.

6.5 Component and signaling cable considerations

Two components (local oscillator and clock chip circuit) on motherboard probably will need an extra local shield placed on it to pass regulatory testing if the components radiate over-limit spurious noise. Hence the mechanical chassis design should also provide sufficient space with height clearance to accommodate this kind of SMT shield/can.

The camera module is also a potential RF noise source of the system, especially when it is located in the proximity of antennas. A mechanical shielding solution – sheet metal, EMI paint, foil, and/or magnesium walls should be considered to isolate the EMI noise from the antennas as shown in Figure 46. Although most of the camera modules equipped with metal shielded enclosure, but the glass which cover the CCD gate, transfer gate may leak or coupling the magnetic field to the nearby traces through the glass aperture.



Fig. 46. Shielded enclosure and loop probe for noise measurement of camera module.

LVDS is now a popular signaling system that can deliver information at very high speed over twisted pair copper cables. LVDS technology uses the voltage difference between two wires to carry signal information for high-speed data transfer through the panel hinge to minimize EMI related problems. In order to minimize the aforementioned EMI problems, we can utilize LVDS cables with the following mechanical recommendations:

1. Make sure that the twisted pair cabling, twin-axial cabling, or flex circuit with closely coupled differential lines is used by grouping members of each pair together.
2. Differential impedance of the cables should be 100 ohms
3. Make sure that the cables used are well shielded
4. Place ground pins between pairs wherever it is possible
5. Connect shielding directly to the connectors of driver and receiver enclosure respectively.

The use of LVDS system must be cautious that most of the LVDS cables have good degree of balance for the fundamental frequency, but the balanced pair becomes unbalanced for those frequencies higher than 10 harmonics when the harmonic signal across the LVDS cable. Therefore it will usually generate the common mode voltage resulting in common mode radiation, and the shield of the LVDS cable become ground return.

The impedance mismatching at DDR2 or DDR3 memory socket usually causes higher noise current distribution around the socket area. These magnetic field may couple to the WWAN module when the shielding effectiveness of WWAN module's shielded enclosure is not adequate as shown in Figures 47-49. Lower impedance will make di/dt increase and dramatically increase the current drawn from supply (not good for the design of power distribution system), while higher impedance will emit more EMI and also become more susceptible to external interference.



Fig. 47. RF module location and nearby field distribution.

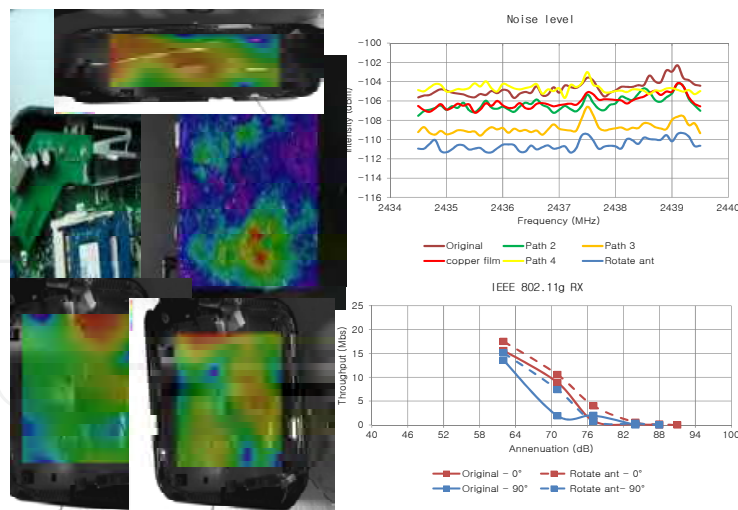


Fig. 48. Embedded antenna mini-coaxial cable and noise distribution.



Fig. 49. Circuit ground and chassis ground.

7. Application of noise budget concept

Finally, we will propose the Noise Budget concept for platform noise suppression. The noise budget for the wireless communication device can be considered as near-field EMC limit. Noise budget is a powerful tool to apply for the wireless product from initial design stage, QA, QC, and all the way to final production testing. For communications community and RF device manufactures, the link budget is established for system planning, therefore most of RF engineers understand that the characteristics of antenna, LNA, mixer play important role for range and coverage extending. However the parameters discussed in link budget are all about signal transmission alone, another important component parameter related to noise level, the Noise Budget, is the missing puzzle for the system integration.

7.1 Introduction to noise budget concept

Since the electronics of the notebook or laptop are the interference source for RF wireless device as discussed earlier. This final section covers some design guidelines and EMI measuring techniques of components, because EMI from internal ICs is also a major contribution to impact the RF performance. The primary purpose here is to address the idea of "Component Noise Budget for Wireless Integration". The concept of noise budget for devices on wireless communication product stems from the link-budget for RF Tx/Rx performance. It also borrows the idea from EMC testing requirements for automobile industry to identify the potential interference sources that might cause safety problem and

thus to provide design guideline for compliance. The noise budget concept helps system designers to manage the EMC issues, as early as possible, such as coupling mechanisms, module placement, grounding, and routing for EMC test. The methodology is intended to develop modular architecture of analysis to accelerate system design and also provide the solutions for potential problems to improve performance in all aspects.

The preliminary goal of this research is to establish the noise budget for components and devices on laptop computer for further RF sensitivity analysis. To utilize the near-field EM scanner to detect the EMI sources on laptop, we can locate the major noise sources in 2D hot-spot distribution graph. From the emission levels and locations of the noisy components, we can figure out their impact on throughput and receiving sensitivity of wireless communication and find the solution to improve performance. The final goal of noise budget, however, is to establish the EMI limits for each digital components related to layout location, it would therefore help designers to choose the appropriate components for optimal placement and cost consideration to meet product requirement. The application of noise budget accompanied with near-field surface scanner not only can locate the EMI source and further to solve the problem, but also can utilize the EM analysis to improve the design efficiency and the performance of wireless communications.

The factors that would affect the receiving performance of a wireless receiver can be illustrate in Figure 50. Table 7 shows the relationship between link budget and noise budget for wireless communication system implementation.

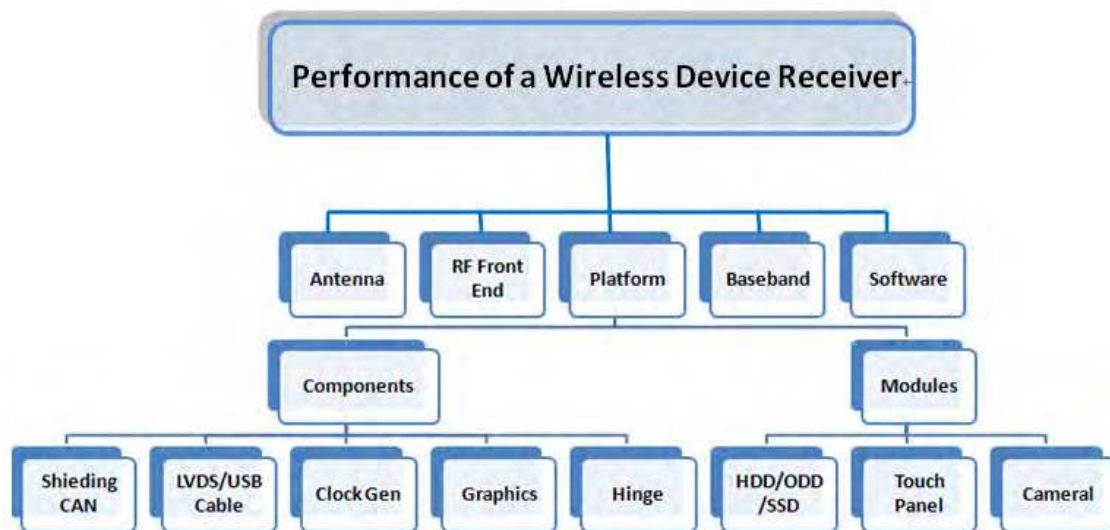


Fig. 50. Factors affecting the receiving performance of a wireless receiver.

PATH LOSS		NOISE LEVEL	
ANTENNA GAIN	-3dB	CPU	
DIPLEXER INSERTION LOSS	-2dB	NORTH BRIDGE(LVDS DRIVER...)	
MISMATCHING LOSS	-0.5dB	MEMORY	
LNA GAIN	+20dB	LVDS SOKET	
LNA NOISE FIGURE	2dB	LVDS FLAT FLEX CABLE	
SAW FILTER LOSS	-2dB	LCD PANEL (T-CON, BACKLIGHT)	
MIXER CONVERSTION LOSS	-0.5dB	TOUCH ME	
SAW FILTER LOSS	-2dB	WEB CAM	
LNA GAIN	+20dB	MINI COAXIAL CABLE FOR RF	
I/Q CONVERSTION LOSS	-8dB	SOUTH BRIDGE	

Table 7. LINK budget (left) vs. NOISE budget (right).

The common interference noise sources on integrated high-speed digital wireless communication product nowadays include: CPU, LCD panel, Memory, digital components, high-speed I/O interconnect, wires and cables, etc. The modules' placement of the test setup is illustrated in Figure 51. The above mentioned noises are usually coupled to nearby sensitive devices through radiation, conduction, or crosstalk. The resulted EMI problem will further degrade the system sensitivity and performance for wireless communications.

After the emitted noise level and corresponding location of each component has been identified, we investigate the effect of component placement on in-band noise level at antenna port and thus the performance of wireless communications by changing distance between antenna and component under test. We can further find the optimal orientation and location of component to improve overall communications performance[9,10].

Because a variety of digital components exist inside laptop computer, we focus on LCD Panel that is equipped in all computers and usually placed in the proximity of antennas. To investigate the effect of various operation modes, (such as off, standby, and key-in alphbat H pattern mode) on noise level at the antenna port, we first arranged the test setup as laptop normally working and scanned the ambient noise.

To clarify the influence of LCD panel noise on antenna port and thus receiving sensitivity, we first fixed the function setting on computer to avoid effect from software's inconsistent running mode. After activating the LCD Panel for various testing mode, we measured the noise spectrum at antenna port to find out the interference frequencies and then use near-field probes to scan the EMI noise from LVDS cables, connectors, and driver ICs of the LCD panel control circuits. Finally, we can investigate the impact of different LCD operation mode on the frequency bands of wireless communications by analyzing the measured throughput results.

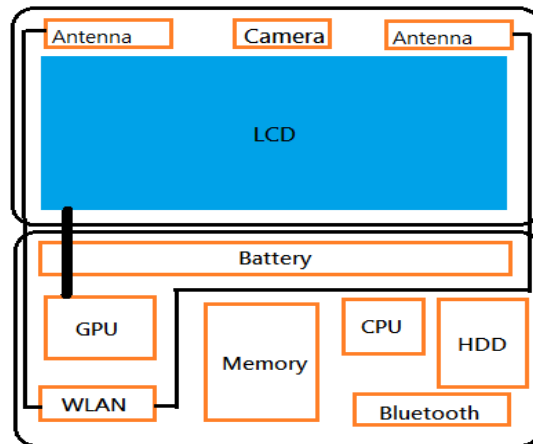


Fig. 51. Internal layout of laptop computer.

7.2 Analysis of platform noise effect from built-in CAMERA module

7.2.1 Test setup for noise level measurement

The system platform noise under investigation is first analyzed by noise floor measurement system. The complete PNS (platform noise measuring system) is composed of shielded box, pre-amplifier, spectrum analyzer, and EUT (Laptop computer). The noise level measuring system and setup for frequency domain is shown in Figure 52.

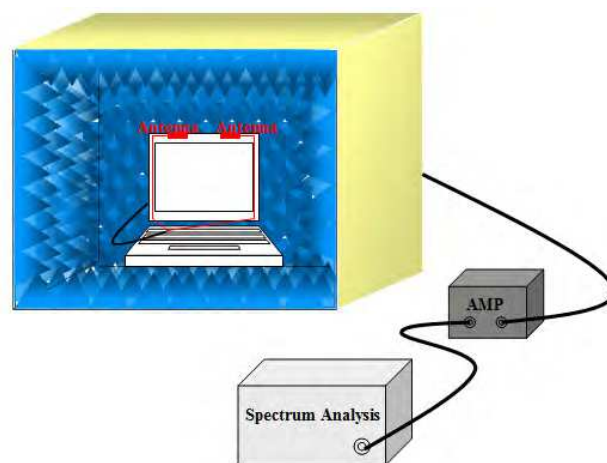


Fig. 52. Setup for antenna port noise level measurement.

Since the CAMERA or CMOS camera module is most adopted to the popular mobile devices like cellular phone or Netbook, we hence focus on EMI analysis of the built-in camera module by application of IEC 61967-2[1].

7.2.2 Test setup for TEM cell measurement[11]

The test setup for TEM cell method in this study is shown in Figure 53. One end of the TEM cell is terminated with a 50 Ω resistance terminator, and the other end is connected to spectrum analyzer via pre-amplifier.

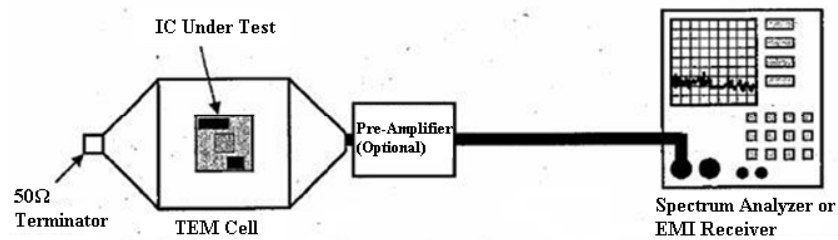


Fig. 53. TEM cell setup for IC or module EMI test.

There are two PCBs with module under test on it and are marked as 1 and 2 shown in Figure 54 and Figure 55. The tested boards for Webcam DUT are driven by USB with clock frequency 48 MHz, and the grounding connection between camera chip and PCB is utilized with wire bonding. The function of module and inner PCB routine for both boards under test are identical except for different number of bonding wires connecting to ground, there are more grounding wires for No. 2 PCB than No.1. The purpose of this measurement is to investigate the effect of multi-point grounding scheme to EMI level. Since the bonding wire is equivalent to inductance, we expect to reduce ground bounce and hence the EMI emission by parallel connection of multiple grounding wires. The connection between camera module and testing board is shown in Figure 56.

The experimental procedure for EMI test using TEM cell is following:

1. Connect the pre-amplifier (if needed) in front of spectrum analyzer at one end, and connect a 50Ω terminator at the other end.
2. Define or identify the four side of TEM cell to place the DUT oriented along all four directions and measure EMI one for each time as shown in Figure 57.
3. Set the measurement frequency range of spectrum analyzer from 150 kHz to 1 GHz.
4. Set the resolution bandwidth of spectrum analyzer around 9 to 10 kHz, and video bandwidth as more than three times of resolution bandwidth to meet the IEC standard specification[12].

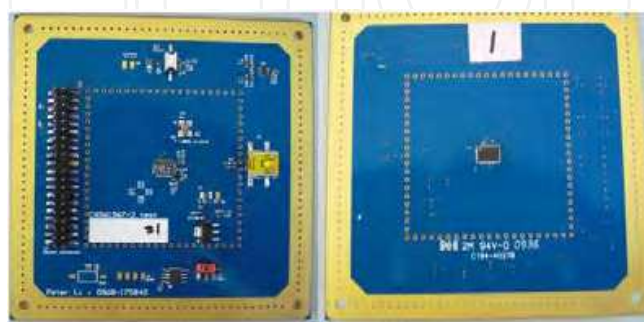


Fig. 54. Physical PCB with CAMERA module marked as NO.1.

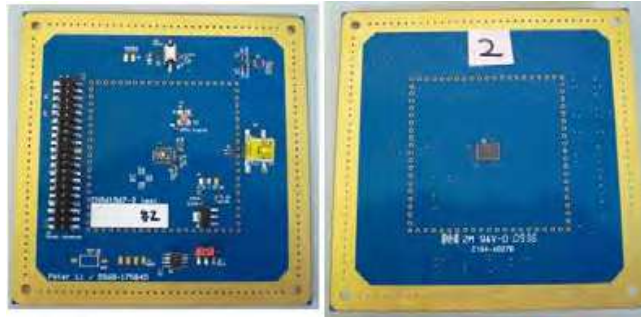


Fig. 55. Physical PCB with CAMERA module marked as NO.2.



Fig. 56. Physical camera connected to testing board.

There were two operation modes for camera module to be analyzed on EMI measurement. The first mode simulates the cellular phone activating the camera module for video communication. In the case of first mode, the camera is simply turned on for full function but does not execute the video file transferring from capturing camera to store on hard disc or memory card. However, the second mode simulates the cellular phone activating the camera module for video recording. In the case of the second mode, the camera is not only activated for full function but also execute the video file transferring from capturing camera to store on hard disc or memory card. The measured results for both operation modes are shown in Table 8 and 9 respectively. Compare the measured results for both operational mode, we can observe the occurring EMI phenomena during video file transferring from capturing camera to storage device. It can be used to find that if the more functions IC executes, would the severe EMI noise be generated or not.

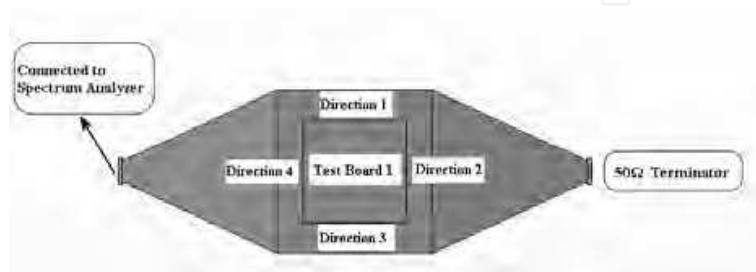


Fig. 57. Definition of 4 directions for TEM cell test orientation.

Direction Board	1	2	3	4
1	9.41 dBuV at 480 MHz	7.37 dBuV at 72 MHz	10.45 dBuV at 480 MHz	6.39 dBuV at 120 MHz
2	8.50 dBuV at 312 MHz	6.44 dBuV at 120 MHz	9.06 dBuV at 312 MHz	7.54 dBuV at 72 MHz

Table 8. Maximum EMI level with corresponding PCB orientation and frequency for video communications mode (mode 1).

Direction Board	1	2	3	4
1	10.63 dBuV at 480 MHz	6.61 dBuV at 720 MHz	11.15 dBuV at 480 MHz	6.39 dBuV at 120 MHz
2	11.14 dBuV at 72 MHz	7.74 dBuV at 960 MHz	9.25 dBuV at 480 MHz	7.32 dBuV at 815 MHz

Table 9. Maximum EMI level with corresponding PCB orientation and frequency for video file transfer mode (mode 2).

7.2.3 Test setup for near-field surface scanning[2,13]

The setup as shown in Figure 58 is to detect the EMI noise from LVDS cables, connectors, and driver ICs of the LCD panel control circuits. From the measured results, we can identify the locations of the significant EMI noise sources.

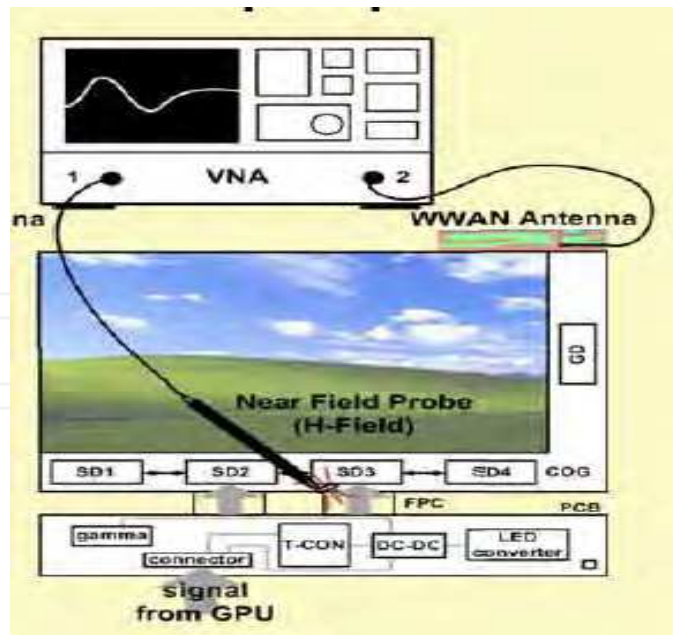


Fig. 58. Setup for LCD panel noise measurement.

7.2.4 Test setup for throughput

The setup of the throughput measurement for the analysis of communications performance in this study is shown in Figure 59. The throughput measurement system consists of WLAN AP (access point), device under test (DUT), attenuator, and Chariot software for data rate control.

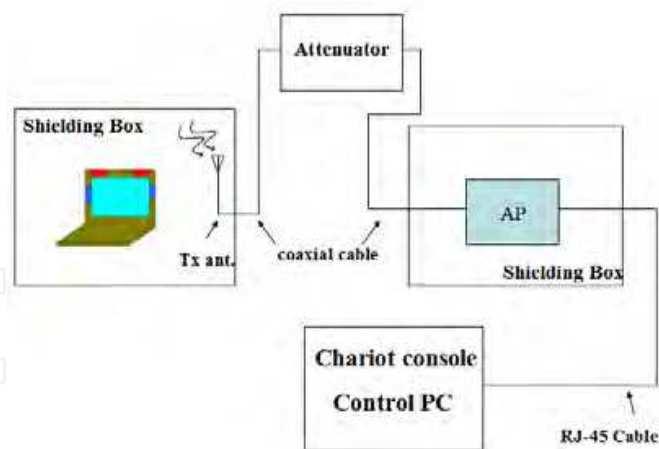


Fig. 59. Setup of throughput measurement system.

7.3 Analysis of measurement results[10-14]

7.3.1 Results of noise level measurement for different LCD panel

Variation of noise level for Camera module at different operation mode is shown in Figure 60. We can observe the significant variation of noise level in 2586~2600MHz frequency range when Camera is activated and operated at Record mode. Since the crystal oscillation

of Camera is 48 MHz, we can conclude that its 50th and 54th harmonics just fall at 2400MHz and 2592MHz, the most significant noise level frequencies, respectively. Therefore, the receiving sensitivity and thus the communications performance in 2.4 GHz band are degraded by the activation of Camera functions.

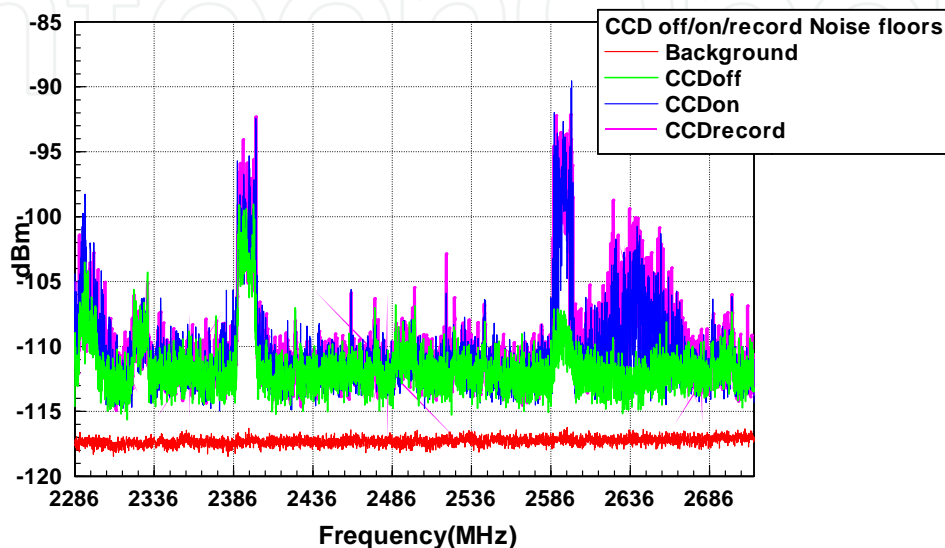
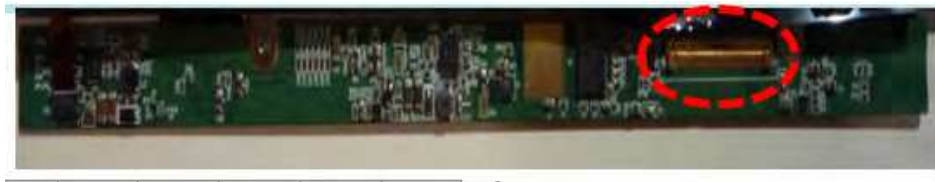


Fig. 60. Noise level for different Camera operation mode.

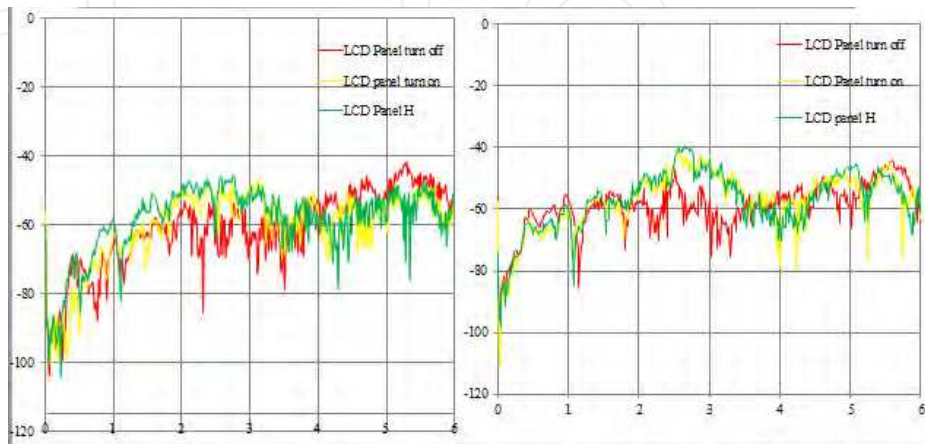
7.3.2 Results of surface-scanning measurement

From the results of noise level measurement, we first obtained the interference frequencies generated from LCD panel. We then used the magnetic near-field probe to observe the noise influence on wireless communication bands via antenna ports from LVDS cables, connectors, and driver ICs of the LCD panel control circuits when LCD panel was set to various operation modes, (such as off, standby, and key-in alphan H pattern mode). Figures 61-63 show the change of transmission coefficients between antenna port and LVDS cables of the LCD panel control circuits. The measured result on left is for horizontal orientation of near-field probe placement, and the one on right is for vertical orientation. When magnetic probe is placed in vertical orientation, it is in parallel with routing traces of LVDS connector and thus results in higher sensitivity. We also observed that the coupling level are much higher for LCD panel operated in standby or key-in alphan H pattern mode than shut off.

Figures 64 and 65 show the change of transmission coefficients between antenna port and driver IC of the LCD panel control circuits. The measured result on left is for horizontal orientation of near-field probe placement, and the one on right is for vertical orientation. We observed that the noises coupled to antenna port are much higher for LCD panel is turned on or displays H pattern mode than shut off, because the control IC is activated.



(a) Measurement position

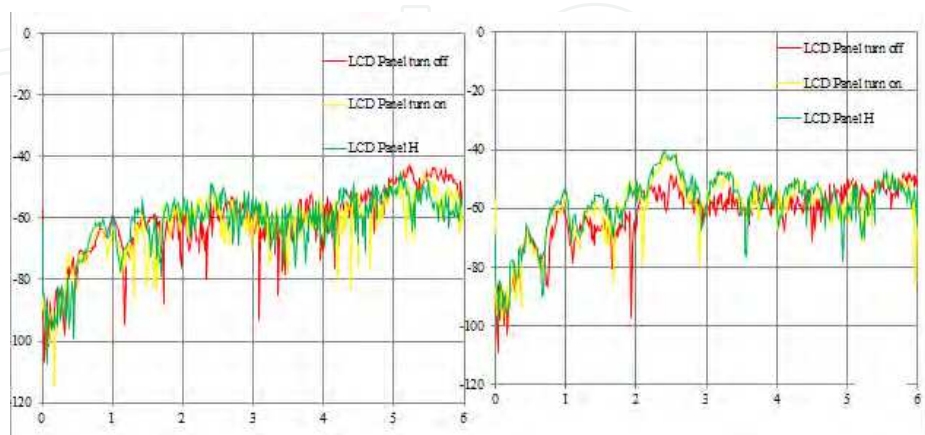


(b) Measured result of S21

Fig. 61. Measurement position (a) and (b) result of LCD Panel control circuit.



(a) Measurement position

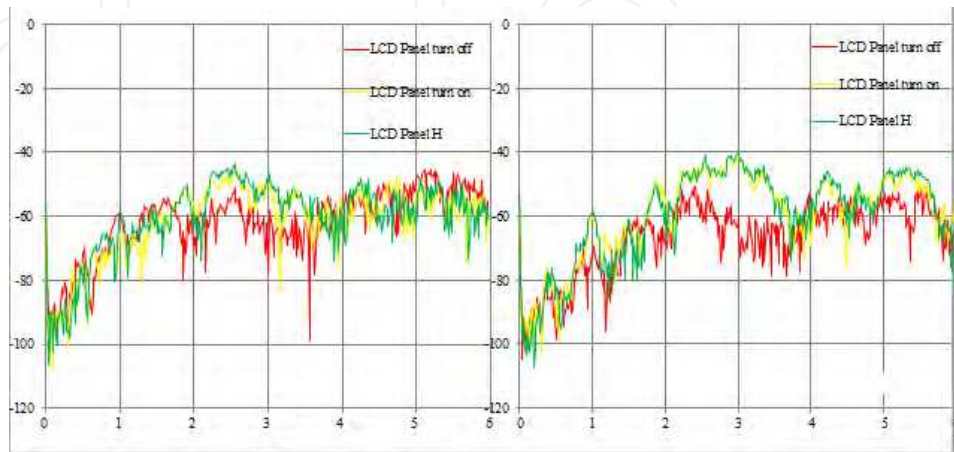


(b) Measured result of S21

Fig. 62. Measurement position (a) and (b) result of LCD Panel control IC.



(a) Measurement position

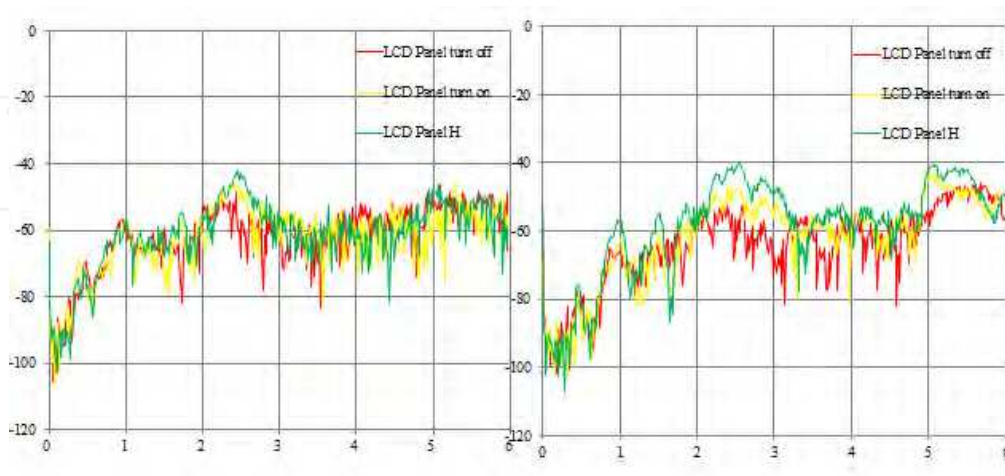


(b) Measured result of S21

Fig. 63. Measurement position (a) and (b) result of LCD Panel control circuit.

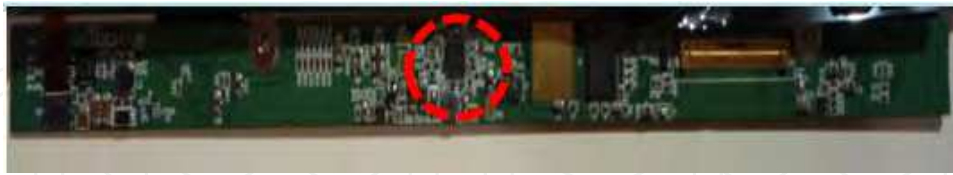


(a) Measurement position

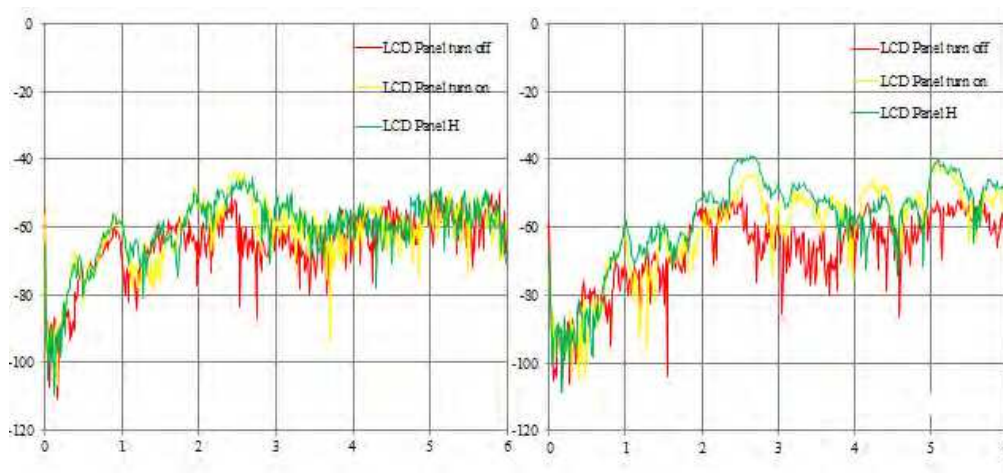


(b) Measured result of S21

Fig. 64. Measurement position (a) and (b) result of LCD Panel control circuit.



(a) Measurement position



(b) Measured result of S21

Fig. 65. Measurement position (a) and (b) result of LCD Panel control circuit.

7.4 Summary

Since the development of IC technologies advancing toward nm processing technology and higher operating frequencies in recent years, the systems of highly integrated high-speed digital circuits and multi-radio modules are now facing the challenge from performance degradation by more complicated electromagnetic noisy environment. With the development of the analyzing and measuring methodologies for this wireless platform noise problem and establishment of noise budget for digital component in the near future, we can provide the EMI coupling mechanism and noise level for each component to help system engineer analyze and design the EMC compliant wireless product in the first beginning as shown in Figure 66 and 67.

TP Noise Budget Fishbone Diagram

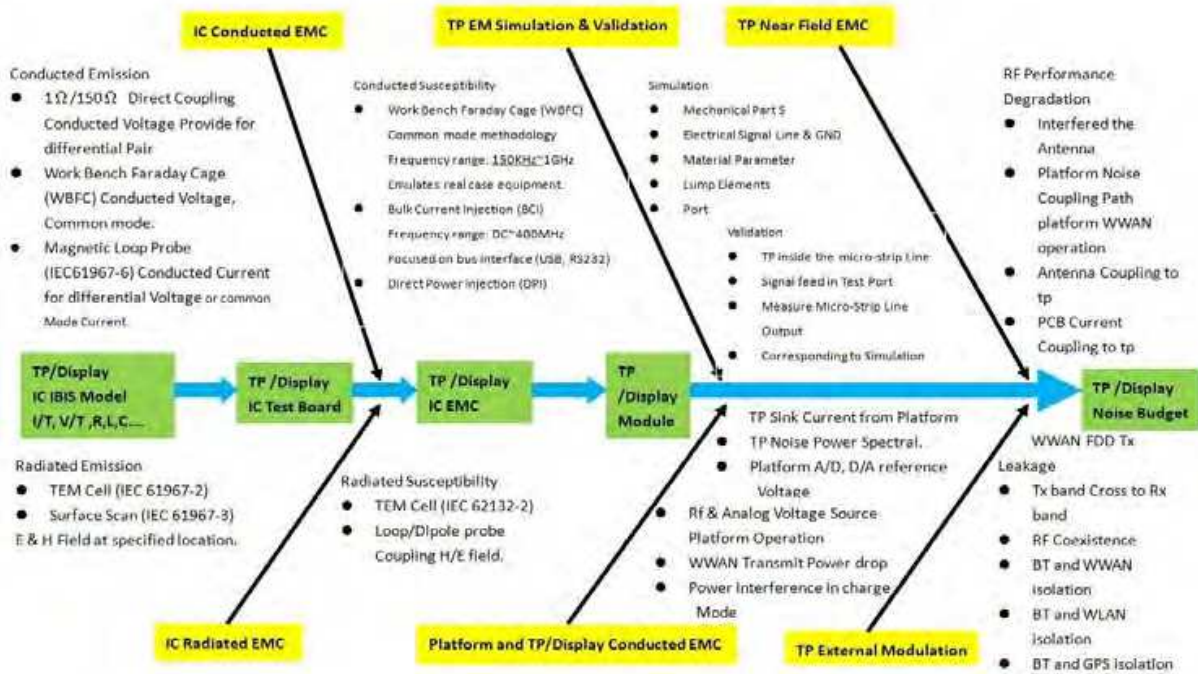


Fig. 66. Noise budget consideration for touch panel.

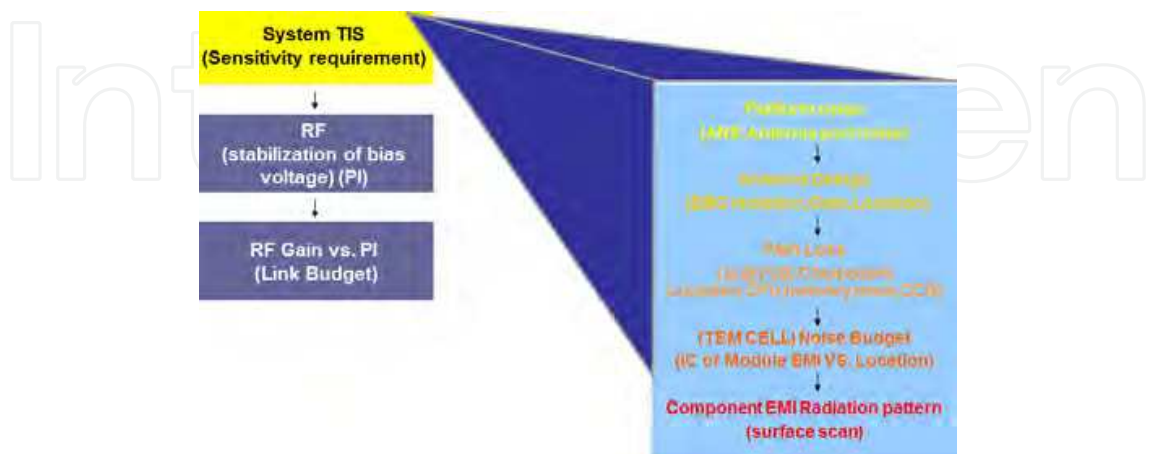


Fig. 67. System view for noise budget.

8. Acknowledgments

The author would like to thank the old friend and research partner Frank Tsai from TRC (Training and Research Company, Taiwan) for his inspiration, technical support and measurement assistance. The author would also like to thank the funding support from BSMI (Bureau of Standards, Metrology and Inspection) and NSC (National Science Council) Taiwan.

9. Reference

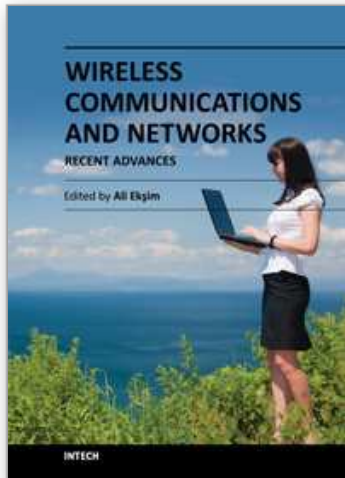
- IEC 61967-2: Integrated circuits - Measurement of electromagnetic emissions, 150 kHz to 1 GHz - Part 2: TEM cell method, International Electrotechnical Commission (IEC), Geneva, Switzerland Int. Std., July 2005.
- IEC 61967-3 Edition 1.0 (2005-06) Integrated circuits - Measurement of electromagnetic emissions, 150 kHz to 1 GHz - Part 3: Measurement of radiated emissions - Surface scan method.
- Test Plan for Mobile Station Over the Air Performance: Method of Measurement for Radiated RF Power and Receiver Performance. Ver. 3.1, CTIA - The Wireless Association, January 2011
- Han-Nien Lin, Ching-Hsien Lin, Tai-Jung Cheng, Min-Chih Liao, *Antenna Effect Analysis of Laptop Platform Noise on WLAN Performance*, PIERS 2009 in Beijing, Session 2A8, March 21-25, 2009
- Han-Nien Lin, Ming-Cheng Chang, Jia-Li Chang, Yung-Chi Tang, Jay-San Chen, *Influence Analysis of LCD Modules Noise on Performance of 802.11b*, 2011 APEMC in Korea, Poster I-6 P55, May 16-19, 2011
- Han-Nien Lin, Ching-Hsien Lin, Ming-Cheng Chang, Yu-Yang Shih, *Analysis of Platform Noise Effect on WWAN*, AMEMC 2010 in Beijing, TH-PM-A1-2: SS-13, April 12-16, 2010
- Nada Golmie, *Coexistence in Wireless Networks: Challenges and System-Level Solutions in the Unlicensed Bands*, Cambridge, 2006
- Han-Nien Lin, Ching-Hsien Lin, Chun-Chi Tang, and Ming-Cheng Chang, *Application of Periodic Structure on the Isolation and Suppression for Notebook Multi-antennas Coupling* PIERS 2010, Xi'an, Proceeding, p.160-164, March 22-26, 2010
- Han-Nien Lin, Chung-Wei Kuo, Jih-Min Liao, Jian-Li Dong, *Design of TEM cell and high sensitive probe for EMI analysis of built-in Webcam module*, 2010 EDAPS in Singapore, THPMTS84, December 07-09, 2010
- Han-Nien Lin, Jing-Ting Cheng, Jian-Li Dong, Jay-San Chen, *Radiated EMI analysis for CMOS Camera module with TEM Cell and Far-field testing*, 2011 APEMC in Korea, Poster I-1 P47, May 16-19, 2011
- Han-Nien Lin, Ming-Feng Cheng, Han-Chang Hsieh, Jay-San Chen, *Design and characteristic analysis of TEM Cell for IC and module EMC testing*, 2011 APEMC in Korea, T-Tu3-5 P103, May 16-19, 2011
- IEC 61967-1: Integrated circuits - Measurement of electromagnetic emissions, 150 kHz to 1 GHz - Part 1: General conditions and definitions, International Electrotechnical Commission (IEC), Geneva, Switzerland Int. Std., March 2002.

Han-Nien Lin, Chung-Shun Chang, Gang-Wei Cao, Cheng-Chang Chen, Jay-San Chen,
Design of High Sensitivity Near-Field Probe and Application on IC EMI Detection, 2011
APEMC in Korea, Poster I-4 P53, May 16-19, 2011

Han-Nien Lin, Tai-jung Cheng, Chih-Min Liao, *Radiated EMI Prediction and Mechanism
Modeling from Measured Noise of Microcontroller*, AMEMC 2010 in Beijing, TH-PM-
A1-4: SS-13, April 12-16, 2010

IntechOpen

IntechOpen



Wireless Communications and Networks - Recent Advances

Edited by Dr. Ali Eksim

ISBN 978-953-51-0189-5

Hard cover, 596 pages

Publisher InTech

Published online 14, March, 2012

Published in print edition March, 2012

This book will provide a comprehensive technical guide covering fundamentals, recent advances and open issues in wireless communications and networks to the readers. The objective of the book is to serve as a valuable reference for students, educators, scientists, faculty members, researchers, engineers and research strategists in these rapidly evolving fields and to encourage them to actively explore these broad, exciting and rapidly evolving research areas.

How to reference

In order to correctly reference this scholarly work, feel free to copy and paste the following:

Han-Nien Lin (2012). Analysis of Platform Noise Effect on Performance of Wireless Communication Devices, *Wireless Communications and Networks - Recent Advances*, Dr. Ali Eksim (Ed.), ISBN: 978-953-51-0189-5, InTech, Available from: <http://www.intechopen.com/books/wireless-communications-and-networks-recent-advances/performance-of-wireless-communication-devices>

INTECH
open science | open minds

InTech Europe

University Campus STeP Ri
Slavka Krautzeka 83/A
51000 Rijeka, Croatia
Phone: +385 (51) 770 447
Fax: +385 (51) 686 166
www.intechopen.com

InTech China

Unit 405, Office Block, Hotel Equatorial Shanghai
No.65, Yan An Road (West), Shanghai, 200040, China
中国上海市延安西路65号上海国际贵都大饭店办公楼405单元
Phone: +86-21-62489820
Fax: +86-21-62489821

© 2012 The Author(s). Licensee IntechOpen. This is an open access article distributed under the terms of the [Creative Commons Attribution 3.0 License](#), which permits unrestricted use, distribution, and reproduction in any medium, provided the original work is properly cited.

IntechOpen

IntechOpen